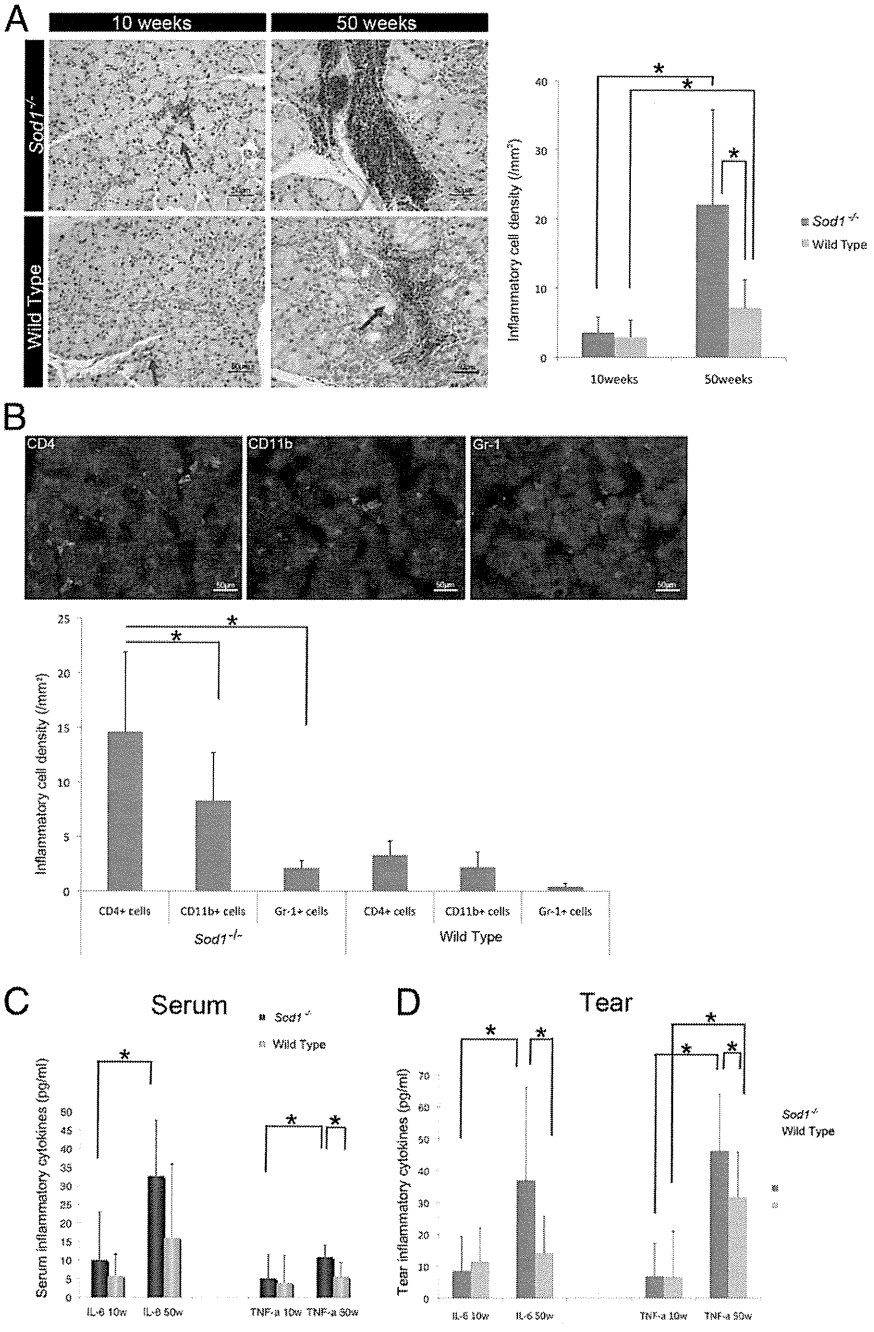

Figure 3. Inflammatory lacrimal gland, serum, and tear alterations in the $Sod1^{-/-}$ and WT mice. **A:** Specimens stained with CD45 in the 10-week-old $Sod1^{-/-}$ and WT mice showed scanty inflammatory cells. Note the relatively more intense staining in the specimen from the $Sod1^{-/-}$ mice at 50 weeks compared with the WT mice. The mean inflammatory cell densities showed a significant timewise increase from 10 weeks to 50 weeks in both the $Sod1^{-/-}$ and WT mice ($P < 0.0001$ and $P = 0.0031$, respectively). Note the significantly higher inflammatory cell density in the $Sod1^{-/-}$ mice at 50 weeks compared with the WT mice ($P < 0.05$). **B:** Specimens from the 50-week-old $Sod1^{-/-}$ mice were stained with anti-CD4, CD11b, and Gr-1 antibodies. Note the CD4-positive cells were dominant among inflammatory cells. The CD4-positive cell density (lower panel) was significantly higher than either the CD11b- or Gr-1–positive cell density. **C:** The mean serum IL-6 concentration in the $Sod1^{-/-}$ mice showed a significant ($P = 0.009$) timewise increase from 10 to 50 weeks. Serum TNF-α levels were also significantly higher ($P = 0.009$) in the $Sod1^{-/-}$ mice at 50 weeks compared with the WT mice at 50 weeks. A significant ($P = 0.016$) timewise increase was seen in the mean TNF-α serum concentration from 10 to 50 weeks in the $Sod1^{-/-}$ mice. **D:** The mean tear IL-6 concentration also showed a significant increase in the $Sod1^{-/-}$ mice from 10 to 50 weeks ($P = 0.002$). Note the significantly higher IL-6 concentration ($P = 0.028$) in the $Sod1^{-/-}$ mice at 50 weeks compared with the WT mice at 50 weeks. The mean tear TNF-α concentrations increased significantly from 10 to 50 weeks in both the $Sod1^{-/-}$ and the WT mice. Note also the significantly higher TNF-α concentration in the $Sod1^{-/-}$ mice compared with the WT mice at 50 weeks ($P < 0.05$). Error bars indicate SD from at least five independent samples per group of three separate experiments. $^*P < 0.05$.

the $Sod1^{-/-}$ mice compared with the WT mice at 50 weeks ($P < 0.05$) (Figure 3D).

The mean tear IL-10, IFN-γ, MCP-1, and IL-12p70 levels did not show significant differences from 10 to 50 weeks in both the $Sod1^{-/-}$ and WT mice. There were also no significant differences in the mean IL-10, IFN-γ, MCP-1, and IL-12p70 concentrations between the WT and the $Sod1^{-/-}$ mice at 50 weeks (data not shown).

IHC and Ultrastructural Evidence of Increased Apoptosis in the Lacrimal Glands

Inflammation in the lacrimal gland has previously been shown to be associated with apoptosis in acinar cells of the lacrimal glands in dry eyes associated with Sjögren syndrome.[32,33] To investigate whether elevated oxidative damage and inflammation status were associated with increased cell death in the lacrimal glands of the current mouse model, we performed immunofluorescence staining with TUNEL and caspase-3 antibodies. TUNEL assay has been used to detect the DNA breakpoints and assess apoptotic cells.[34] Lacrimal gland samples from all $Sod1^{-/-}$ mice at 50 weeks showed marked positive staining with TUNEL for apoptotic cells (572.21 cells/mm^2) compared with specimens from $Sod1^{-/-}$ mice at 10 weeks (110.05 cells/mm^2) and WT mice at 50 weeks (247.21 cells/mm^2). Increased positive staining was also observed for the WT mice lacrimal gland specimens from

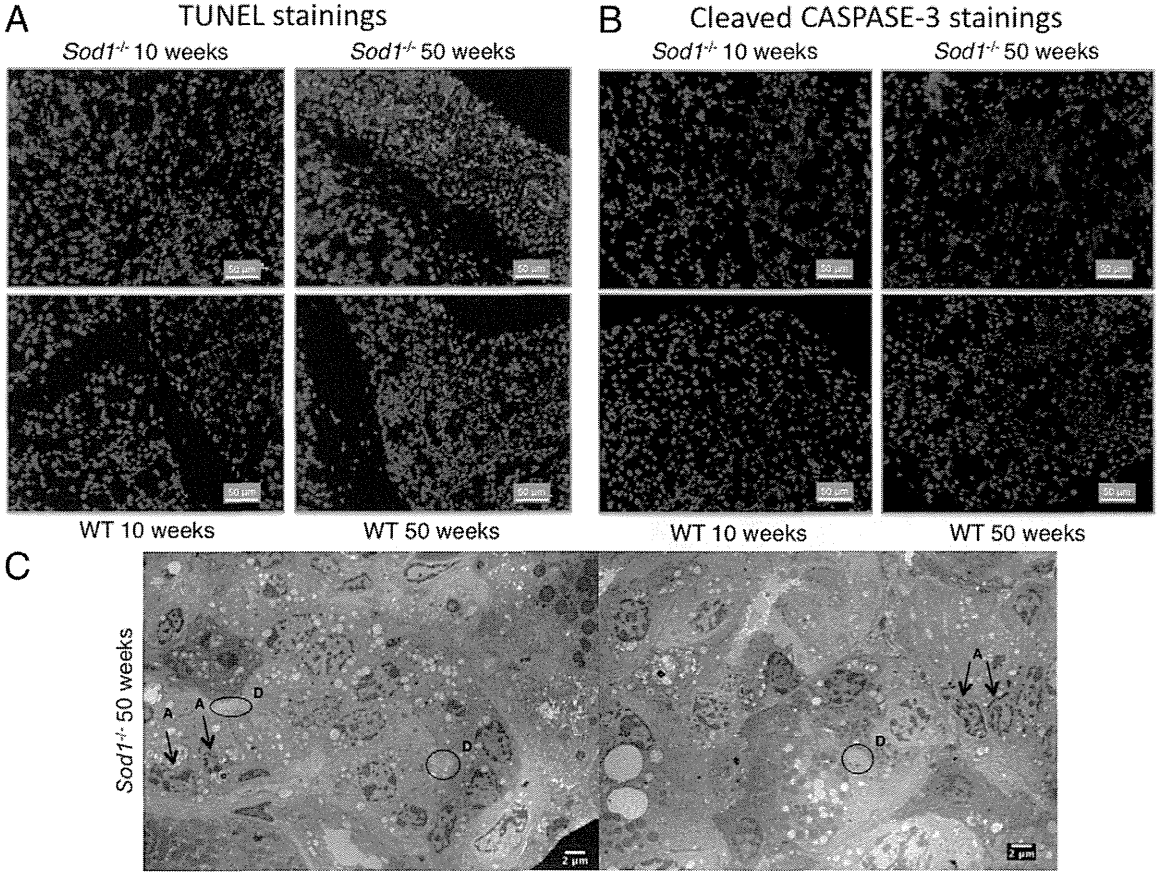

Figure 4. IHC and ultrastructural evidence of apoptosis in the lacrimal glands. **A:** Lacrimal gland samples from all *Sod1*$^{-/-}$ mice at 50 weeks showed marked positive staining with TUNEL for apoptotic cells (572.21 cells/mm^2) compared with specimens from *Sod1*$^{-/-}$ mice at 10 weeks (110.05 cells/mm^2) and WT mice at 50 weeks (247.21 cells/mm^2). Increased positive staining was also observed for the WT mice lacrimal gland specimens from 10 weeks (27.11 cells/mm^2) to 50 weeks (247.21 cells/mm^2). **B:** Specimens from the *Sod1*$^{-/-}$ mice at 50 weeks displayed relatively more positive staining (178.63 cells/mm^2) with caspase-3 antibodies for apoptotic cells compared with specimens from *Sod1*$^{-/-}$ mice at 10 weeks (65.39 cells/mm^2) and WT at 50 weeks (116.43 cells/mm^2). **C:** Note the evidence for apoptosis (**A**; **arrows**) in acinar epithelial cells by transmission electron microscopy. Specimens from the *Sod1*$^{-/-}$ mice at 50 weeks exclusively and prominently displayed fragmentation and shrinkage of the nuclei, cytoplasmic vacuole formation, and loss of nuclear membranes. The areas indicated by circles and ellipses correspond to the lacrimal gland acinar ducts (D). Images are representatives of at least five independent samples per group.

10 weeks (27.11 cells/mm^2) to 50 weeks (247.21 cells/mm^2) (Figure 4A). We also performed cleaved caspase-3 staining by immunofluorescence. Caspase-3 has been regarded to be an important mediator of apoptosis.[35] Specimens from the *Sod1*$^{-/-}$ mice at 50 weeks displayed relatively more positive staining (178.63 cells/mm^2) with caspase-3 antibodies for apoptotic cells compared with specimens from *Sod1*$^{-/-}$ mice at 10 weeks (65.39 cells/mm^2) and WT mice at 50 weeks (116.43 cells/mm^2) (Figure 4B). We also sought for evidence of apoptosis in acinar epithelial cells by transmission electron microscopy. A total of 88.2% of the specimens from the *Sod1*$^{-/-}$ mice at 50 weeks displayed marked fragmentation and shrinkage of the nuclei, cytoplasmic vacuole formation, and loss of nuclear membranes (Figure 4C). Such changes were not observed in specimens of WT mice at 10 and 50 weeks and *Sod1*$^{-/-}$ mice at 10 weeks (data not shown).

Lacrimal Gland Fibrosis and Related Morphologic Alterations in the Sod1$^{-/-}$ *and WT Mice*

As shown in Figure 5A, lacrimal glands removed from the 10-week-old WT and *Sod1*$^{-/-}$ mice showed normal ductal and acinar cell morphologic features and lobular architecture separated by interlobular connective tissue. At 50 weeks, lacrimal glands in the *Sod1*$^{-/-}$ mice exclusively developed a severe inflammatory response with inflammatory cells invading the interlobular spaces surrounding both acinar and ductal cells. Lobular atrophy due to atrophy of the acinar cells, interlobular and periductal fibrosis, and interlobular duct dilatation were observed. Slight periductal and interlobular fibrosis together with a few inflammatory cells were also noted in the WT mice lacrimal gland specimens. To further describe the extent of fibrosis, Mallory staining was performed, which stains areas of fibrosis with a dark blue color.[20,21] Almost no interlobular fibrosis was observed in both *Sod1*$^{-/-}$ and WT mice at 10 weeks. Extensive interlobular and periacinar Mallory staining was observed in the lacrimal gland specimens of all *Sod1*$^{-/-}$ mice at 50 weeks, with some slight interlobular positive staining observed in the age-matched WT mice (Figure 5B).

To quantify the lacrimal gland acinar unit densities, we counted the number of acinar units within a fixed area for all samples. We observed that there were no statistically significant differences between the mean acinar unit densities

of *Sod1*$^{-/-}$ (780.89 ± 150.05 units/μm^2) and WT (794.39 ± 78.75 units/μm^2) mice at 10 weeks. There was a decrease in the mean acinar unit densities from 10 weeks to 50 weeks in both *Sod1*$^{-/-}$ and WT mice (Figure 5C). The mean acinar unit density in the lacrimal gland specimens of the *Sod1*$^{-/-}$ mice at 50 weeks (379.72 ± 92.78 units/μm^2) was significant lower than the acinar unit density in the WT mice at 50 weeks (514.58 ± 47.43 units/μm^2) ($P < 0.001$).

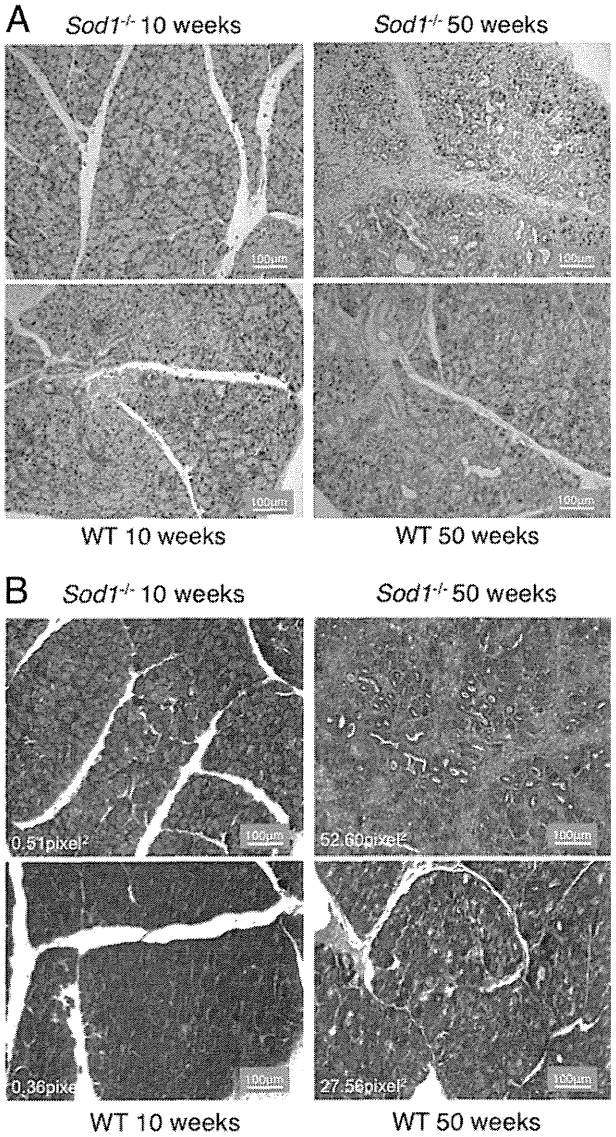

Evaluation of EMT in Lacrimal Glands of Sod1$^{-/-}$ *and WT Mice*

To further study the processes involved in lacrimal gland fibrosis, we decided to investigate the presence of EMT in the lacrimal gland. Lacrimal gland specimens were immunostained with epithelial and mesenchymal markers, namely, E-cadherin and α-SMA. Type I collagen was expressed in basement membranes of acinar cells in both *Sod1*$^{-/-}$ and WT mice (Figure 6, A–D). In eyes of 50-week-old *Sod1*$^{-/-}$ mice, disruption of basement membrane was observed (Figure 6D). α-SMA immunostaining was observed in the periacinar areas of the epithelial cells in all specimens (Figure 6, E–H). The number of α-SMA–positive cells was significantly higher in the 50-week-old *Sod1*$^{-/-}$ mice compared with the WT mice. On the other hand, positive E-cadherin staining was observed in the intercellular junctions between adjacent lacrimal gland acinar cells (Figure 6, I–L), and expression was lower in the 50-week-old *Sod1*$^{-/-}$ mice compared with the WT mice (Figure 6L). To further quantify the mRNA expression levels of EMT-related markers, SYBR Green–based quantitative real-time PCR was performed. The expression of Snail, which is an inducer of EMT, was significantly higher in the 50-week-old *Sod1*$^{-/-}$ mice than in 50-week-old WT and 10-week-old *Sod1*$^{-/-}$ mice (Figure 6M). The expression of α-SMA, which is a mesenchymal cell marker, was significantly higher in the 50-week-old *Sod1*$^{-/-}$ mice than in 50-week-old WT mice (Figure 6N). The expression of E-cadherin, which is an epithelial cell marker, was significantly lower in the 50-week-old *Sod1*$^{-/-}$ mice than the 50-week-old WT mice, the 10-week-old *Sod1*$^{-/-}$ mice, and the 10-week-old WT mice (Figure 6O). The expression level of the α-SMA/E-cadherin ratio was significantly higher in the 50-week-old *Sod1*$^{-/-}$ mice than the 50-week-old WT mice, 10-week-old *Sod1*$^{-/-}$ mice, and 10-week-old WT mice (Figure 6P).

Figure 5. Evidence of further morphologic alterations in the *Sod1*$^{-/-}$ and WT mice lacrimal glands. **A:** Lacrimal glands from the 10-week-old WT and *Sod1*$^{-/-}$ mice showed normal ductal and acinar cell morphologic features. At 50 weeks, lacrimal glands in the *Sod1*$^{-/-}$ mice exclusively developed a severe inflammatory response, with inflammatory cells invading the interlobular spaces surrounding both the acinar and ductal cells. Lobular atrophy due to atrophy of the acinar cells, interlobular and periductal fibrosis, and interlobular duct dilatations were observed. Slight periductal and interlobular fibrosis together with a few inflammatory cells were also noted in the WT mice lacrimal gland specimens. **B:** Extensive interlobular and periacinar fibrosis was observed in the lacrimal gland specimens of all *Sod1*$^{-/-}$ mice at 50 weeks, with some slight interlobular positive staining in the age-matched WT mice. Images in **A** and **B** are representatives of at least five independent samples per group. **C:** No statistically significant differences were found between the mean acinar unit densities of the *Sod1*$^{-/-}$ and WT mice at 10 weeks. There was a timewise decrease in the mean acinar unit densities from 10 weeks to 50 weeks in both *Sod1*$^{-/-}$ and WT mice ($P < 0.0001$). The mean acinar unit density in the lacrimal gland specimens of the *Sod1*$^{-/-}$ mice at 50 weeks was significant lower then the acinar unit density in the WT mice at 50 weeks (*$P < 0.001$, Mann-Whitney test). Data in **C** represents the mean and SD of combined data from seven mice per group and are representative of three separate experiments.

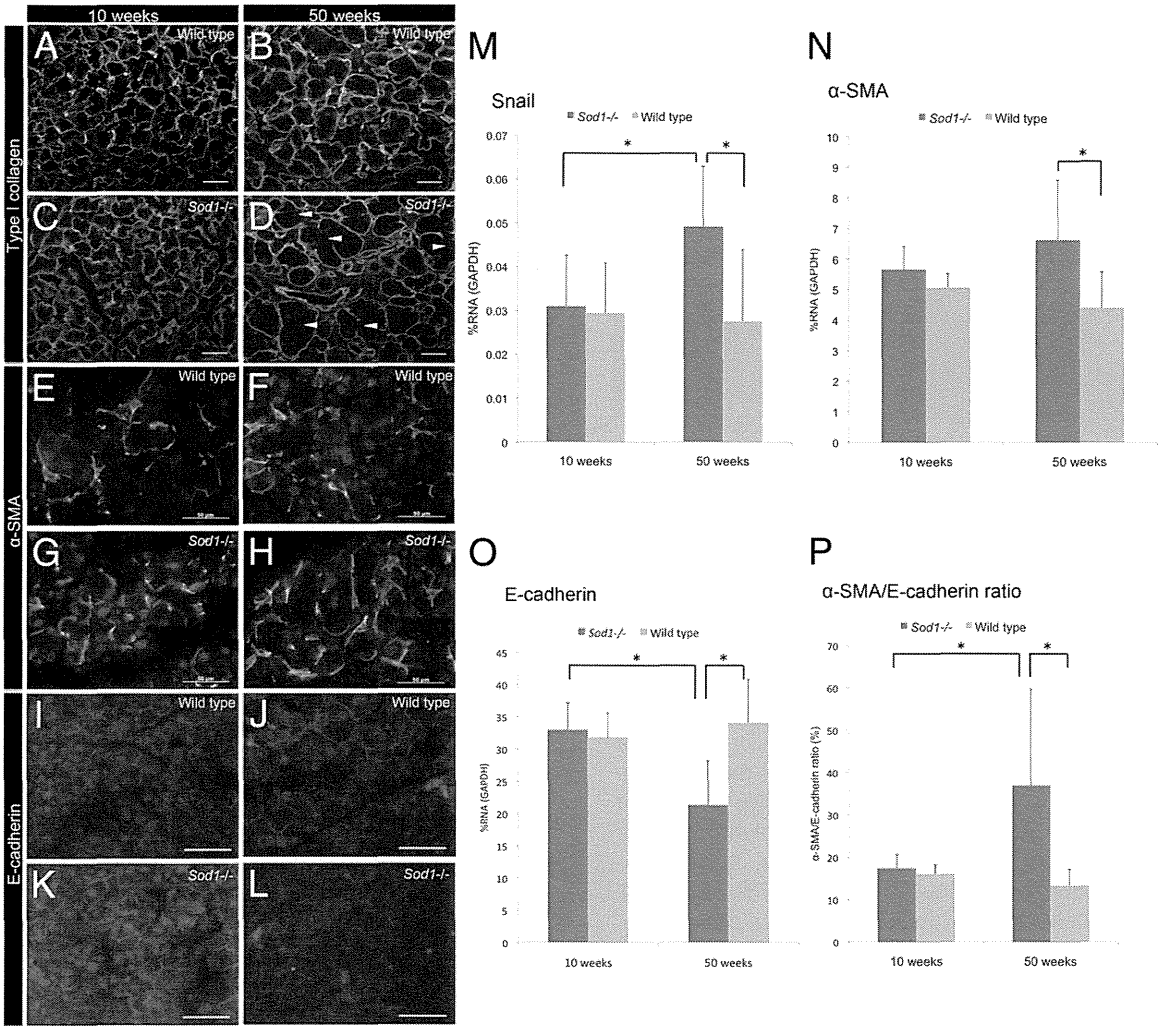

Figure 6. IHC and quantitative transcript evaluation of EMT in the lacrimal gland of WT and *Sod1*$^{-/-}$ mice. IHC using anti–collagen type I antibody (**A–D**) revealed disruption of basement membrane in 50-week-old *Sod1*$^{-/-}$ mice (**D**). **Arrowhead** showed the location of basement membrane disruption (**D**). IHC staining of α-SMA (**E–H**) in 50-week-old *Sod1*$^{-/-}$ mice (**H**) increased compared with 50-week-old WT mice (**F**). On the other hand, IHC staining of E-cadherin (**I–L**) in 50-week-old *Sod1*$^{-/-}$ mice (**L**) decreased compared with 50-week-old WT mice (**J**). **M:** Quantitative real-time PCR revealed that Snail expression in 50-week-old *Sod*$^{-/-}$ mice was higher than 50-week-old WT mice and 10-week-old *Sod1*$^{-/-}$ mice. **N:** α-SMA expression in 50-week-old *Sod1*$^{-/-}$ mice was higher than 50-week-old WT mice. **O:** E-cadherin expression in 50-week-old *Sod*$^{-/-}$ mice was lower than in 50-week-old WT mice, 10-week-old WT mice, and 10-week-old *Sod1*$^{-/-}$ mice. **P:** The α-SMA/E-cadherin ratio in 50-week-old *Sod*$^{-/-}$ mice was higher than in 50-week-old WT mice, 10-week-old *Sod1*$^{-/-}$ mice, and 10-week-old WT mice. *$P < 0.05$.

Ultrastructural Evidence for EMT in the Lacrimal Glands

Electron microscopy observation of lacrimal gland in the 50-week-old *Sod1*$^{-/-}$ mice revealed loss of polarity of acinar epithelial cells, which is feature of EMT (Figure 7). Higher magnification of electron microscopy also revealed the presence of secretory vesicles and microvilli toward the interstitial area with evidence of increased collagen lay-down (Figure 7).

Lacrimal Gland Secretory Functions Decrease Overtime in the Sod1$^{-/-}$ *Mice, Leading to Ocular Surface Disease*

We measured aqueous tear production with the cotton thread test and divided the values by the respective mouse weights at 10 and 50 weeks. Weight-adjusted aqueous tear production measurements were significantly lower in the *Sod1*$^{-/-}$ ($n = 17$) mice compared with the age- and sex-matched WT ($n = 14$) mice at 10 weeks and 50 weeks (10-week-old *Sod1*$^{-/-}$ mice: 0.094 ± 0.077 μL/g; 50-week-old *Sod1*$^{-/-}$ mice: 0.050 ± 0.035 μL/g; 10-week-old WT mice: 0.175 ± 0.112 μL/g; and 50-week-old WT mice: 0.168 ± 0.089 μl/g) as shown in Figure 8A. A significant decrease of tear production from 10 to 50 weeks was also observed in the *Sod1*$^{-/-}$ mice ($P = 0.026$) (Figure 8A). On stimulation with pilocarpine, the tear secretion tended to decrease from 10 to 50 weeks in the *Sod1*$^{-/-}$ mice with a tendency to increase in the WT mice without statistical significance. However, pilocarpine-stimulated tear secretion was significantly lower ($P = 0.0364$) in the *Sod1*$^{-/-}$ mice at 50 weeks (0.034 ± 0.009 μL/g) compared with the WT mice (0.079 ± 0.010

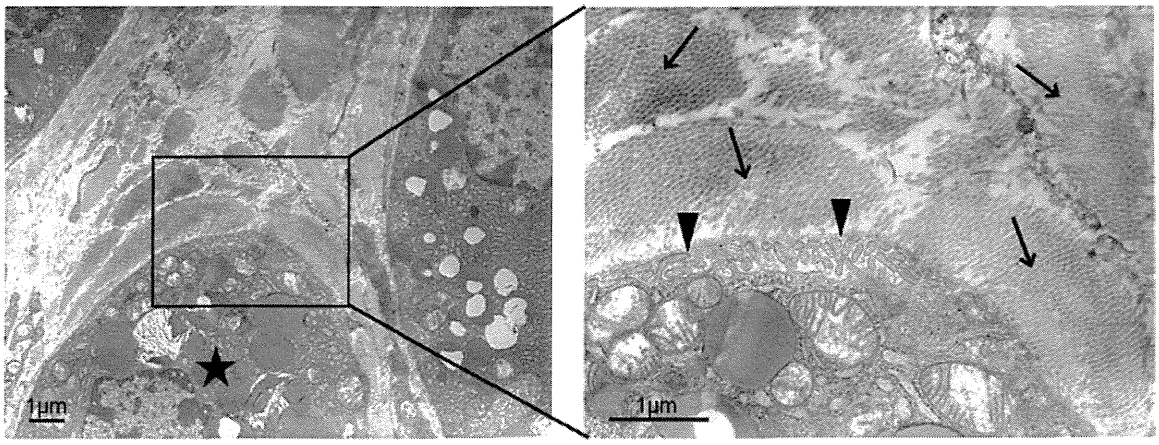

Figure 7. Electron microscopy of lacrimal gland in 50-week-old *Sod1*$^{-/-}$ mice. Note the loss of polarity of the acinar epithelial cell (**star**) with the microvilli (**arrowhead**) and secretary vesicles facing the mesenchymal area, which has abundant collagen fibers (**arrow**). **Right panel** is an enlargement of the boxed region of the **left panel**.

μL/g) (Figure 8B). Not only the aqueous tear but also the total protein secretion measured at 50 weeks was significantly less in the *Sod1*$^{-/-}$ mice (0.920 ± 0.968 μg/mL/g/min) compared with the WT mice (3. 433 ± 2.467 μg/mL/g/min) (P = 0.024) (Figure 8C). Cotton thread test measurements revealed mean tear quantity values of 0.083 ± 0.067 mm/g and 0.124 ± 0.065 mm/g in the *Sod1*$^{-/-}$ mice and WT mice, respectively. We also found that 87.5% of the *Sod1*$^{-/-}$ mice and 5.9% of the WT mice at 50 weeks were below the cutoff value. In addition, 5.4% of the SOD1 knockout mice and 2.7% of the WT mice at 10 weeks had dry eye disease (data not shown).

We observed, by transmission electron microscopy examination, that the secretory vesicles in the lacrimal gland acinar cells appeared as gray-black, electron-dense, round-oval bodies. We noted a relative accumulation of secretory vesicles in the acinar epithelia in *Sod1*$^{-/-}$ mice from 10 to 50 weeks (Figure 8D). After quantifying the density of secretory vesicles, we noted a significant accumulation of secretory vesicles in the acinar epithelial cells from 10 weeks (558.14 ± 90.04 vesicles per frame) to 50 weeks (709.80 ± 91.25 vesicles per frame) in the *Sod1*$^{-/-}$ mice (P = 0.03). The number of secretory vesicles did not change significantly in the WT mice from 10 weeks (284 ± 90.82 vesicles per frame) to 50 weeks (460.60 ± 125.46 vesicles per frame) as shown in Figure 8E (P = 0.076). The differences in the number of secretory vesicles per area between the *Sod1*$^{-/-}$ mice and the WT mice at 10 weeks were statistically significant (P = 0.006). The mean number of secretory vesicles was also significantly higher in the *Sod1*$^{-/-}$ mice at 50 weeks than the WT mice at 50 weeks (P = 0.003) (Figure 8E).

Decreased tear output has been shown to be associated with establishment of a dry eye ocular surface milieu, leading to ocular surface epithelial damage.[7] The mean fluorescein staining score in the *Sod1*$^{-/-}$ mice was significantly higher (P = 0.001) than the WT mice at 10 (2 ± 1 points) and 50 weeks (2.21 ± 1.42 points). The mean fluorescein score also showed a significant increase (P = 0.026) from 10 (4.3 ± 1.06 points) to 50 weeks (5.5 ± 1.76 points) in the *Sod1*$^{-/-}$ mice (Figure 8F). Representative corneal fluorescein stainings at 50 weeks are shown in Figure 8G. Whereas corneal epithelium from the WT mice displayed no or minimal punctate staining, the corneal epithelium in all *Sod1*$^{-/-}$ mice had marked corneal epithelial damage.

Evidence for Presence of Age-Related Increase of Oxidative Stress and Morphologic Alterations in Human Lacrimal Glands

Human samples were studied under institutional review board permission at Keio University School of Medicine. H&E and Mallory staining revealed acinar unit atrophy; interstitial, periacinar, and periductal fibrosis; and cystic duct dilatation with inflammatory cells in the lacrimal gland specimens from older individuals, which were not observed in the younger individuals (see Supplemental Figure S1 at *http://ajp.amjpathol.org*). Staining of the lacrimal gland specimens in the older individuals with anti–4-HNE antibodies showed marked staining of acinar units, indicating increased lipid oxidative damage compared with the scanty staining observed in the younger group of individuals. There was also comparably more and prominent staining for 8-OHdG, indicating extensive DNA damage in the lacrimal gland specimens of the older individuals compared with the younger individuals. Lacrimal gland specimens from older individuals also showed marked infiltration with CD45-positive inflammatory cells compared with the younger individuals.

Discussion

Previous experimental animal studies proposed that *Sod1*$^{-/-}$ caused an elevated oxidative stress status, resulting in various aging phenotypes, such as muscle[36] and skin atrophy,[37] bone weakness,[38] fat liver deposits, hepatic carcinoma,[39] and hemolytic anemia.[40,41] In humans, oxidative stress has been reported to be involved in many systemic diseases, including Parkinson's disease,[42] Alzheimer's disease,[43–45] amyotrophic lateral

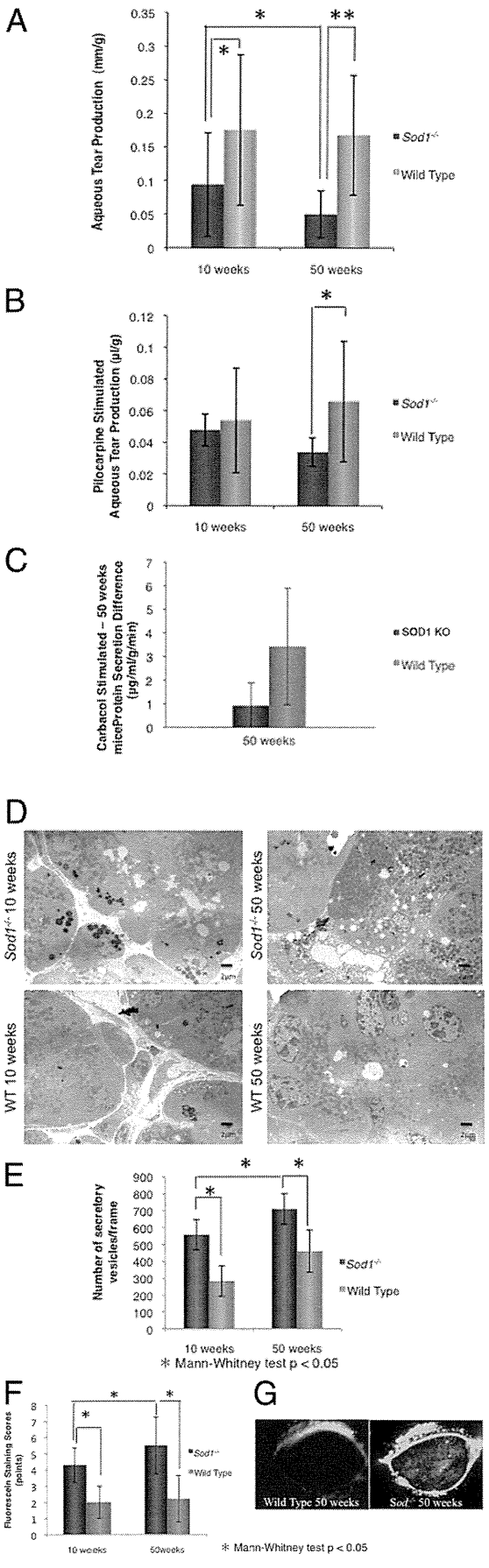

sclerosis,[46] cardiovascular diseases,[47,48] cancer,[39,49,50] and ischemic disorders due to oxygen reperfusion injury followed by hypoxia.[51,52] Oxygen free radicals and antioxidant systems have been demonstrated to be potentially important in the pathogenesis of ocular diseases, such as cataract,[53] uveitis,[54] retinopathy of prematurity,[55] AMD,[56] keratitis,[57] keratoconus, and bullous keratopathy.[58] The role and relation of oxidative stress in the pathogenesis of dry eye disease have not been investigated in an aging animal model or in humans before.

The *Sod1*$^{-/-}$ mouse has been shown by us to be a good model for studying retinal oxidative stress changes, which were found to be strongly related to the morphologic and functional retinal alterations similar to human AMD.[4]

In this study, we investigated whether histopathologic alterations existed in the lacrimal glands of the *Sod1*$^{-/-}$ mice and whether these changes translated into functional glandular disturbances, causing dry eye disease. Because the amount and activity of *Sod1* are the highest among the three isozymes in humans, it seemed reasonable to hypothesize that the lack of *Sod1* would accelerate oxidative stress and age-related pathologic changes in the lacrimal glands of the *Sod1*$^{-/-}$ mice.[59]

We observed extensive lipid and DNA oxidative stress damage in the lacrimal gland acinar epithelia, which appeared to increase with aging from 10 to 50 weeks in both the knockout and WT mice. The DNA damage seemed to be more extensive in the old *Sod1*$^{-/-}$ mice compared with the old WT mice. Elevation of serum 8-OHdG provided additional evidence on general cellular DNA damage in the *Sod1*$^{-/-}$ mice. Oxidative stress-related cellular DNA damage has previously been demonstrated in heart, brain, muscles, liver, red blood cells, and other organs in several age-related diseases, including cardiovascular disorders, neurodegenerative diseases, and cancer.[25,39,43,47,48,60,61]

Our observations suggested an accelerated oxidative lipid and DNA damage in the lacrimal glands of *Sod1*$^{-/-}$

Figure 8. Changes in lacrimal gland secretory functions and corneal epithelial damage over time in the *Sod1*$^{-/-}$ and WT mice. **A:** Weight-adjusted aqueous tear production measurements were significantly lower in the *Sod1*$^{-/-}$ mice compared with the WT mice at 10 weeks and 50 weeks. A significant timewise decrease of tear production from 10 to 50 weeks was also observed in the *Sod1*$^{-/-}$ mice (P = 0.026). **B:** There is significantly lower tear production with pilocarpine stimulation in the *Sod1*$^{-/-}$ mice at 50 weeks. **C:** At 50 weeks the amount of protein produced, after carbachol stimulation, by the *Sod1*$^{-/-}$ mouse group was lower compared with the WT group. **D:** There is marked timewise accumulation of secretory vesicles in the lacrimal glands of the *Sod1*$^{-/-}$ mice. **E:** There is significant accumulation of secretory vesicles in the acinar epithelial cells from 10 weeks to 50 weeks in the *Sod1*$^{-/-}$ mice (P = 0.030). The number of secretory vesicles did not change significantly in the WT mice from 10 weeks to 50 weeks (P = 0.076). The differences in the number of secretory vesicles/area between the *Sod1*$^{-/-}$ and WT mice at 10 weeks were statistically significant (P = 0.006); the mean number of secretory vesicles was considerably higher in the *Sod1*$^{-/-}$ mice at 50 weeks than the WT mice at 50 weeks (P = 0.003). **F:** Changes in corneal epithelial damage scores assessed by fluorescein staining in the *Sod1*$^{-/-}$ and WT mice. A statistically significant timewise increase in the fluorescein staining score was observed in the *Sod1*$^{-/-}$ mice. Note the significantly higher scores in the *Sod1*$^{-/-}$ mice compared with WT mice at 50 weeks. **G:** Representative photomicrographs of fluorescein staining test in the 50-week-old mice. Note the extensive corneal epithelial damage in the *Sod1*$^{-/-}$ mouse compared with the WT mouse at 50 weeks. Error bars indicate SD from at least five independent samples per group of three separate experiments.

mice compared with WT mice, also strengthening our belief that these changes might have very well resulted from accumulation of reactive oxygen species in the lacrimal gland cellular architecture, especially in mitochondria. Accumulation of reactive oxygen species has been shown and linked to mitochondrial alterations in humans and animal models of age-related diseases[44,46,62–65] with striking disturbances in the mitochondrial architecture, including mitochondrial swelling, rupture of membranes, and disruption of cristae changes, which were also observed in our *Sod1*$^{-/-}$ mice.

Such alterations in the mitochondrial cytoskeleton have also been linked to activation of apoptotic signals, initiating cell death.[66–69] We showed an increase in the process of apoptotic cell death over time in the lacrimal glands of the *Sod1*$^{-/-}$ and WT mice by confirming increased TUNEL and caspase-3 staining with a comparatively greater extent of staining in the old *Sod1*$^{-/-}$ compared with old WT mice. Fragmentation of nuclei and vacuolar changes in the lacrimal gland acinar epithelia provided further ultrastructural evidence of the presence of apoptosis as a possible mechanism of cell death in this study. This observation differs from that of Hashizume et al,[70] who found both apoptosis and necrosis in the retina of the *Sod1*$^{-/-}$ mice. We believe this difference in cell death mechanisms is attributable to light exposure protected ocular anatomical location of the lacrimal gland.

We think increased caspase-3 staining overtime in our knockout mice is an important observation because even a small amount of caspase-3 activation has been shown to be sufficient to initiate genomic DNA breakdown, leading to apoptotic cell death.[71] Nonapoptotic functions of caspase-3 include induction of inflammation through lymphocyte proliferation and antigen presentation.[72,73]

We noted an altered "inflammation status" in the lacrimal gland tissue with significant increases in the lacrimal gland inflammatory cell infiltrate densities in both *Sod1*$^{-/-}$ and WT mice overtime, with the difference becoming more significant in the old knockout than the old WT mice. These observations were consistent with previous studies that showed increased focal infiltrates in lacrimal glands with a variety of inflammatory cells with aging.[74–79] In this study, we observed that the inflammatory cells were predominantly CD4$^+$ T cells at 50 weeks in the *Sod1*$^{-/-}$ mice. We previously reported that the conjunctival and lacrimal gland tissues of the *Sod1*$^{-/-}$ mice also became simultaneously infiltrated with CD45 and CD4$^+$ cells from 30 weeks and predominate the lacrimal gland and conjunctival tissues densely at 50 weeks (without evidence of corneal infiltration), with a simultaneous decrease in goblet cell density, Muc5ac mRNA expressions in RT-PCR, and a decrease in tear quantity from approximately 30 weeks becoming significant at 50 weeks (unpublished data). The lacrimal/conjunctival or the corneal tissues of the *Sod1*$^{-/-}$ mice lacked any marked infiltration at 10 weeks, which excludes the possibility of an inflammatory process being the cause of corneal staining observed in the mice at that age. The few inflammatory cells observed were cells tracking or patrolling the lacrimal gland tissues.

Inflammatory cells have been reported to release several cytokines that play an important role by initiating or further adding to the process of apoptotic cell death.[80–82] Likewise, lacrimal gland epithelial cells in an inflamed environment have been shown to express cytokines in dry eye disease and with aging.[83] This study noted significant increases in two cytokines in the old knockout mice compared with the old WT mice: TNF-α and IL-6. TNF-α has indeed been demonstrated in increased amounts in the lacrimal glands of old but not young mice.[11] Increased TNF-α and IL-6 concentrations have also been shown in dry eye syndromes in previous studies.[7,8,11,84–86] The reported roles for TNF-α include induction of inflammation and cell death, and those for IL-6 include induction of inflammation and fibrosis.[83,87–90] The cytokine alterations observed in this study go along well and are consistent with increased inflammatory cell density in our knockout mice model with aging. Again, consistent with the cytokine alterations, we observed an exaggerated fibrosis of the interstitium in the lacrimal glands of the old *Sod1*$^{-/-}$ mice, which was also comparatively more extensive than the lacrimal glands of the old WT mice.

To extensively study the mechanisms involved in the process of fibrosis, we decided to investigate the changes in EMT markers in both WT and *Sod1*$^{-/-}$ mice. EMT plays a crucial role not only in physiologic conditions, such as embryonic development or tissue remodeling, but also in pathologic conditions, such as cancer and organ fibrosis.[91] Pathologic EMT has been reported to be induced by inflammatory cytokines, reactive oxygen species, hypoxia, UV irradiation, and nicotine.[92,93] EMT-inducing inflammatory cytokines include transforming growth factor β, TNF-α, and IL-6,[94,95] the last two of which were significantly increased in tears and serum of the 50-week-old *Sod1*$^{-/-}$ mice. We believe that these inflammatory changes invited EMT with increased collagen lay down, fibrosis, and loss of glandular acinar units in due course. A previous report also showed that the EMT in lacrimal gland was caused by human ocular chronic graft-*versus*-host disease.[96]

Draper et al found increased inflammatory cell infiltration, acinar atrophy, and fibrosis among age-related alterations in lacrimal glands of rats.[76] In the human lacrimal glands, Damato et al and Obata et al described atrophy of secretory acini, periductal fibrosis, and increased inflammatory cell infiltration with aging,[75,78,79] similar to our observations, which included interlobular fibrosis, cystic dilatation of ducts, atrophy of secretory acini, and inflammatory cell infiltration and were more prominent and extensive in the knockout mice in this study. Attempts to quantify these phenotypic alterations in the lacrimal gland acinar units revealed significant decreases in the secretory acinar unit density in the *Sod1*$^{-/-}$ mice, a parameter that we thought would reflect the process of acinar atrophy. Apoptosis of acinar and ductal epithelia of the lacrimal glands along with glandular atrophy have been previously proposed as a possible mechanism for the impairment of glandular secretory function.[33,97] A striking ultrastructural observation was related to the extensive accumulation of secretory vesi-

cles in the lacrimal gland acinar epithelia in the *Sod1*$^{-/-}$ mice overtime compared with the WT mice. These observations suggest that the lacrimal glands may be unable to secrete tears in the presence of marked mitochondrial alterations in the *Sod1*$^{-/-}$ mice because mitochondria are the cellular powerhouses important for normal tear secretions.[27,98] Whereas the mitochondria in the lacrimal glands of the *Sod1*$^{-/-}$ mice showed striking ultrastructural alterations, which might lead to decreased tear production, further evidence from future studies simultaneously looking into lacrimal gland ATP levels, mitochondrial membrane potentials, and Ca^{++} currents across lacrimal gland acinar epithelial membranes may provide essential proof of whether the mitochondrial dysfunction in the presence of phenotypic mitochondrial alterations is linked to tear production decrease or not. Surprisingly, we found a significant decrease in the weight-adjusted aqueous tear production, pilocarpine-stimulated tear output, and total protein secretion capacity of the lacrimal gland in the old *Sod1*$^{-/-}$ mice compared with the old WT mice.

Decreased aqueous tear and protein output by the lacrimal gland and increased corneal epithelial damage are universally well-known features of the dry eye disease in animals and humans.[99–101] The higher corneal epithelial damage observed in the *Sod1*$^{-/-}$ mice reflects both the detrimental effects of decreased tear production on the ocular surface and possible oxidative stress damage on cell membrane lipids. *Sod1* is an abundant Cu- and Zn-containing protein present in cytosol,[67] nucleus, peroxisomes, and mitochondrial intermembrane space.[62,102] Its primary function is to act as an antioxidant enzyme, lowering the steady-state concentrations of superoxide.[103] Our results suggest that oxidative stress is not merely an associated phenomenon but may be an integral and primary cause of age-related dry eye disease in the *Sod1*$^{-/-}$ mice model. Adding further to our surprise were the similar observations in young and old human lacrimal gland specimens showing extensive lipid and DNA oxidation, inflammatory cell infiltration, fibrosis, and cystic duct dilatation in the aged individuals compared with the young individuals. Whereas the lacrimal gland samples from the human young and old individuals showed striking differences in relation to increased staining for oxidative stress markers and increased fibrosis and glandular atrophy, which were more prominent in the old individuals, tear function differences still need to be proven, although previous reports indicated a decrease in tear secretion with aging.[104–106] Future studies looking into differences among reflex tearing, total tear protein secretion, and histopathologic differences of lacrimal gland samples obtained for diagnostic purposes in young and old individuals may increase our understanding of whether the *Sod1*$^{-/-}$ mice are relevant to the human disease or may be useful to identify novel therapies for age-related dry eye disease.

We were unable to disclose when exactly the sequence of mechanistic events resulted in the phenotype observed in the lacrimal glands of the SOD1 knockout mice, which possibly led to dry eye and ocular surface disease. Relevant lacrimal gland pathophysiological and tear function examinations in the *Sod1*$^{-/-}$ mice performed more frequently in future studies will provide useful information.

In conclusion, we demonstrated that the lack of *Sod1* led to increased oxidative lipid and DNA damage, increased $CD4^+$ T-cell inflammation, and EMT in the lacrimal glands of the current mouse model, interfering with glandular secretory functions, which resulted in dry eyes and translated into an ocular surface disease.

Acknowledgments

We thank Dr. Yutaka Imamura for advice on experimental design and help with subsequent analysis, Yasumasa Sasaki and Samantha Koto Ward for their initial experimental assistance during the early stages of this work, and Yusuke Ozawa (Tokyo Metropolitan Institute of Gerontology) for his logistic support in maintaining the knockout mice.

References

1. Droge W: Free radicals in the physiological control of cell function. Physiol Rev 2002, 82:47–95
2. Crapo JD, Oury T, Rabouille C, Slot JW, Chang LY: Copper,zinc superoxide dismutase is primarily a cytosolic protein in human cells. Proc Natl Acad Sci U S A 1992, 89:10405–10409
3. Fridovich I: Superoxide anion radical (O2-.), superoxide dismutases, and related matters. J Biol Chem 1997, 272:18515–18517
4. Imamura Y, Noda S, Hashizume K, Shinoda K, Yamaguchi M, Uchiyama S, Shimizu T, Mizushima Y, Shirasawa T, Tsubota K: Drusen, choroidal neovascularization, and retinal pigment epithelium dysfunction in SOD1-deficient mice: a model of age-related macular degeneration. Proc Natl Acad Sci U S A 2006, 103:11282–11287
5. Friedman DS, O'Colmain BJ, Munoz B, Tomany SC, McCarty C, de Jong PT, Nemesure B, Mitchell P, Kempen J: Prevalence of age-related macular degeneration in the United States. Arch Ophthalmol 2004, 122:564–572
6. Smith JA, Albeitz J, Begley C, Caffery B, Nichols K, Schaumberg D, Schein O: The epidemiology of dry eye disease: report of the Epidemiology Subcommittee of the International Dry Eye WorkShop. Ocul Surf 2007, 5:93–107
7. Pflugfelder SC, Jones D, Ji Z, Afonso A, Monroy D: Altered cytokine balance in the tear fluid and conjunctiva of patients with Sjögren's syndrome keratoconjunctivitis sicca. Curr Eye Res 1999, 19:201–211
8. Stern ME, Pflugfelder SC: Inflammation in dry eye. Ocul Surf 2004, 2:124–130
9. Barabino S, Chen W, Dana MR: Tear film and ocular surface tests in animal models of dry eye: uses and limitations. Exp Eye Res 2004, 79:613–621
10. Suwan-apichon O, Rizen M, Rangsin R, Herretes S, Reyes JM, Lekhanont K, Chuck RS: Botulinum toxin B-induced mouse model of keratoconjunctivitis sicca. Invest Ophthalmol Vis Sci 2006, 47:133–139
11. Zoukhri D: Effect of inflammation on lacrimal gland function. Exp Eye Res 2006, 82:885–898
12. Niederkorn JY, Stern ME, Pflugfelder SC, De Paiva CS, Corrales RM, Gao J, Siemasko K: Desiccating stress induces T cell-mediated Sjögren's syndrome-like lacrimal keratoconjunctivitis. J Immunol 2006, 176:3950–3957
13. Song XJ, Li DQ, Farley W, Luo LH, Heuckeroth RO, Milbrandt J, Pflugfelder SC: Neurturin-deficient mice develop dry eye and keratoconjunctivitis sicca. Invest Ophthalmol Vis Sci 2003, 44:4223–4229
14. Ikegami T, Suzuki Y, Shimizu T, Isono K, Koseki H, Shirasawa T: Model mice for tissue-specific deletion of the manganese superox-

ide dismutase (MnSOD) gene. Biochem Biophys Res Commun 2002, 296:729–736
15. Dursun D, Wang M, Monroy D, Li DQ, Lokeshwar BL, Stern ME, Pflugfelder SC: A mouse model of keratoconjunctivitis sicca. Invest Ophthalmol Vis Sci 2002, 43:632–638
16. Botelho SY, Hisada M, Fuenmayor N: Functional innervation of the lacrimal gland in the cat: origin of secretomotor fibers in the lacrimal nerve. Arch Ophthalmol 1966, 76:581–588
17. Ruskell GL: The distribution of autonomic post-ganglionic nerve fibres to the lacrimal gland in monkeys. J Anat 1971, 109:229–242
18. Walcott B, Claros N, Patel A, Brink PR: Age-related decrease in innervation density of the lacrimal gland in mouse models of Sjögren's syndrome. Adv Exp Med Biol 1998, 438:917–923
19. Dotti G, Savoldo B, Takahashi S, Goltsova T, Brown M, Rill D, Rooney C, Brenner M: Adenovector-induced expression of human-CD40-ligand (hCD40L) by multiple myeloma cells: a model for immunotherapy. Exp Hematol 2001, 29:952–961
20. Anderson GG: Tissue processing, microtomy and paraffin sections. Theory and practice of histological techniques. Edited by JD Bancroft. Edinburgh, Churchill–Livingstone, 1996, pp. 47–68
21. Hopwood J: Fixation and fixtative. Theory and practice of histological techniques. Edited by Bancroft JD. Edinburgh, Churchill–Livingstone, 1996, pp. 23–46
22. Zeisberg EM, Tarnavski O, Zeisberg M, Dorfman AL, McMullen JR, Gustafsson E, Chandraker A, Yuan X, Pu WT, Roberts AB, Neilson EG, Sayegh MH, Izumo S, Kalluri R: Endothelial-to-mesenchymal transition contributes to cardiac fibrosis. Nat Med 2007, 13:952–961
23. Zeisberg M, Kalluri R: Fibroblasts emerge via epithelial-mesenchymal transition in chronic kidney fibrosis. Front Biosci 2008, 13:6991–6998
24. Kojima T, Chang JH, Azar DT: Proangiogenic role of ephrinB1/EphB1 in basic fibroblast growth factor-induced corneal angiogenesis. Am J Pathol 2007, 170:764–773
25. Shiihara T, Kato M, Ichiyama T, Takahashi Y, Tanuma N, Miyata R, Hayasaka K: Acute encephalopathy with refractory status epilepticus: bilateral mesial temporal and claustral lesions, associated with a peripheral marker of oxidative DNA damage. J Neurol Sci 2006, 250:159–161
26. Dalle-Donne I, Rossi R, Colombo R, Giustarini D, Milzani A: Biomarkers of oxidative damage in human disease. Clin Chem 2006, 52: 601–623
27. Wallace DC, Fan W: Energetics, epigenetics, mitochondrial genetics. Mitochondrion 2009, 10:12–31
28. Hensley K, Robinson KA, Gabbita SP, Salsman S, Floyd RA: Reactive oxygen species, cell signaling, and cell injury. Free Radic Biol Med 2000, 28:1456–1462
29. Halliday GM: Inflammation, gene mutation and photoimmunosuppression in response to UVR-induced oxidative damage contributes to photocarcinogenesis. Mutat Res 2005, 571:107–120
30. Dahl M, Bauer AK, Arredouani M, Soininen R, Tryggvason K, Kleeberger SR, Kobzik L: Protection against inhaled oxidants through scavenging of oxidized lipids by macrophage receptors MARCO and SR-AI/II. J Clin Invest 2007, 117:757–764
31. Pulido R, Cebrian M, Acevedo A, de Landazuri MO, Sanchez-Madrid F: Comparative biochemical and tissue distribution study of four distinct CD45 antigen specificities. J Immunol 1988, 140:3851–3857
32. Tsubota K, Fujita H, Tadano K, Onoda N, Tsuzaka K, Takeuchi T: Abnormal expression and function of Fas ligand of lacrimal glands and peripheral blood in Sjögren's syndrome patients with enlarged exocrine glands. Clin Exp Immunol 2002, 129:177–182
33. Tsubota K, Fujita H, Tsuzaka K, Takeuchi T: Quantitative analysis of lacrimal gland function, apoptotic figures: Fas and Fas ligand expression of lacrimal glands in dry eye patients, Exp Eye Res 2003, 76:233–240
34. Wyllie AH: Glucocorticoid-induced thymocyte apoptosis is associated with endogenous endonuclease activation. Nature 1980, 284: 555–556
35. Nicholson DW, Ali A, Thornberry NA, Vaillancourt JP, Ding CK, Gallant M, Gareau Y, Griffin PR, Labelle M, Lazebnik YA, et al.: Identification and inhibition of the ICE/CED-3 protease necessary for mammalian apoptosis. Nature 1995, 376:37–43
36. Muller FL, Song W, Liu Y, Chaudhuri A, Pieke-Dahl S, Strong R, Huang TT, Epstein CJ, Roberts LJ, 2nd, Csete M, Faulkner JA, Van Remmen H: Absence of CuZn superoxide dismutase leads to elevated oxidative stress and acceleration of age-dependent skeletal muscle atrophy. Free Radic Biol Med 2006, 40:1993–2004
37. Murakami K, Inagaki J, Saito M, Ikeda Y, Tsuda C, Noda Y, Kawakami S, Shirasawa T, Shimizu T: Skin atrophy in cytoplasmic SOD-deficient mice and its complete recovery using a vitamin C derivative. Biochem Biophys Res Commun 2009, 382:457–461
38. Nojiri H, Saita Y, Morikawa D, Kobayashi K, Tsuda C, Miyazaki T, Saito M, Marumo K, Yonezawa I, Kaneko K, Shirasawa T, Shimizu T: Cytoplasmic superoxide causes bone fragility due to low turnover osteoporosis and impaired collagen cross-linking. J Bone Miner Res 2011, 26:2682–2694
39. Elchuri S, Oberley TD, Qi W, Eisenstein RS, Jackson Roberts L, Van Remmen H, Epstein CJ, Huang TT: CuZnSOD deficiency leads to persistent and widespread oxidative damage and hepatocarcinogenesis later in life. Oncogene 2005, 24:367–380
40. Iuchi Y, Okada F, Onuma K, Onoda T, Asao H, Kobayashi M, Fujii J: Elevated oxidative stress in erythrocytes due to a SOD1 deficiency causes anaemia and triggers autoantibody production. Biochem J 2007, 402:219–227
41. Iuchi Y, Okada F, Takamiya R, Kibe N, Tsunoda S, Nakajima O, Toyoda K, Nagae R, Suematsu M, Soga T, Uchida K, Fujii J: Rescue of anaemia and autoimmune responses in SOD1-deficient mice by transgenic expression of human SOD1 in erythrocytes. Biochem J 2009, 422:313–320
42. Schapira AH, Tolosa E: Molecular and clinical prodrome of Parkinson disease: implications for treatment. Nat Rev Neurol 2010, 6:309–317
43. Higgins GC, Beart PM, Shin YS, Chen MJ, Cheung NS, Nagley P: Oxidative stress: emerging mitochondrial and cellular themes and variations in neuronal injury. J Alzheimers Dis 2010, 20(Suppl 2): S453–S473
44. Du H, Guo L, Fang F, Chen D, Sosunov AA, McKhann GM, Yan Y, Wang C, Zhang H, Molkentin JD, Gunn-Moore FJ, Vonsattel JP, Arancio O, Chen JX, Yan SD: Cyclophilin D deficiency attenuates mitochondrial and neuronal perturbation and ameliorates learning and memory in Alzheimer's disease. Nat Med 2008, 14:1097–1105
45. Reddy PH: Amyloid precursor protein-mediated free radicals and oxidative damage: implications for the development and progression of Alzheimer's disease. J Neurochem 2006, 96:1–13
46. Deng HX, Shi Y, Furukawa Y, Zhai H, Fu R, Liu E, Gorrie GH, Khan MS, Hung WY, Bigio EH, Lukas T, Dal Canto MC, O'Halloran TV, Siddique T: Conversion to the amyotrophic lateral sclerosis phenotype is associated with intermolecular linked insoluble aggregates of SOD1 in mitochondria. Proc Natl Acad Sci U S A 2006, 103:7142–7147
47. Milei J, Forcada P, Fraga CG, Grana DR, Iannelli G, Chiariello M, Tritto I, Ambrosio G: Relationship between oxidative stress, lipid peroxidation, and ultrastructural damage in patients with coronary artery disease undergoing cardioplegic arrest/reperfusion. Cardiovasc Res 2007, 73:710–719
48. Nojiri H, Shimizu T, Funakoshi M, Yamaguchi O, Zhou H, Kawakami S, Ohta Y, Sami M, Tachibana T, Ishikawa H, Kurosawa H, Kahn RC, Otsu K, Shirasawa T: Oxidative stress causes heart failure with impaired mitochondrial respiration. J Biol Chem 2006, 281:33789–33801
49. Reuter S, Gupta SC, Chaturvedi MM, Aggarwal BB: Oxidative stress, inflammation, and cancer: how are they linked? Free Radic Biol Med 2010, 49:1603–1616
50. Pavlides S, Tsirigos A, Migneco G, Whitaker-Menezes D, Chiavarina B, Flomenberg N, Frank PG, Casimiro MC, Wang C, Pestell RG, Martinez-Outschoorn UE, Howell A, Sotgia F, Lisanti MP: The autophagic tumor stroma model of cancer: role of oxidative stress and ketone production in fueling tumor cell metabolism. Cell Cycle 2010, 9:3485–3505
51. Chong ZZ, Shang YC, Hou J, Maiese K: Wnt1 neuroprotection translates into improved neurological function during oxidant stress and cerebral ischemia through AKT1 and mitochondrial apoptotic pathways. Oxid Med Cell Longev 2010, 3:153–165
52. Ying W, Xiong ZG: Oxidative stress and NAD+ in ischemic brain injury: current advances and future perspectives. Curr Med Chem 2010, 17:2152–2158
53. Spector A: Oxidative stress-induced cataract: mechanism of action. FASEB J 1995, 9:1173–1182

54. Gritz DC, Montes C, Atalla LR, Wu GS, Sevanian A, Rao NA: Histochemical localization of superoxide production in experimental autoimmune uveitis. Curr Eye Res 1991, 10:927–931
55. Niesman MR, Johnson KA, Penn JS: Therapeutic effect of liposomal superoxide dismutase in an animal model of retinopathy of prematurity. Neurochem Res 1997, 22:597–605
56. Winkler BS, Boulton ME, Gottsch JD, Sternberg P: Oxidative damage and age-related macular degeneration. Mol Vis 1999, 5:32
57. Alio JL, Artola A, Serra A, Ayala MJ, Mulet ME: Effect of topical antioxidant therapy on experimental infectious keratitis. Cornea 1995, 14:175–179
58. Behndig A, Karlsson K, Johansson BO, Brannstrom T, Marklund SL: Superoxide dismutase isoenzymes in the normal and diseased human cornea. Invest Ophthalmol Vis Sci 2001, 42:2293–2296
59. Behndig A, Svensson B, Marklund SL, Karlsson K: Superoxide dismutase isoenzymes in the human eye. Invest Ophthalmol Vis Sci 1998, 39:471–475
60. Uchiyama S, Shimizu T, Shirasawa T: CuZn-SOD deficiency causes ApoB degradation and induces hepatic lipid accumulation by impaired lipoprotein secretion in mice. J Biol Chem 2006, 281:31713–31719
61. Barber SC, Mead RJ, Shaw PJ: Oxidative stress in ALS: a mechanism of neurodegeneration and a therapeutic target. Biochim Biophys Acta 2006, 1762:1051–1067
62. Sturtz LA, Diekert K, Jensen LT, Lill R, Culotta VC: A fraction of yeast Cu,Zn-superoxide dismutase and its metallochaperone CCS, localize to the intermembrane space of mitochondria: a physiological role for SOD1 in guarding against mitochondrial oxidative damage. J Biol Chem 2001, 276:38084–38089
63. Balaban RS, Nemoto S, Finkel T: Mitochondria, oxidants, and aging. Cell 2005, 120:483–495
64. Borthwick GM, Johnson MA, Ince PG, Shaw PJ, Turnbull DM: Mitochondrial enzyme activity in amyotrophic lateral sclerosis: implications for the role of mitochondria in neuronal cell death. Ann Neurol 1999, 46:787–790
65. Kuwahara H, Horie T, Ishikawa S, Tsuda C, Kawakami S, Noda Y, Kaneko T, Tahara S, Tachibana T, Okabe M, Melki J, Takano R, Toda T, Morikawa D, Nojiri H, Kurosawa H, Shirasawa T, Shimizu T: Oxidative stress in skeletal muscle causes severe disturbance of exercise activity without muscle atrophy. Free Radic Biol Med 2010, 48:1252–1262
66. Chwa M, Atilano SR, Reddy V, Jordan N, Kim DW, Kenney MC: Increased stress-induced generation of reactive oxygen species and apoptosis in human keratoconus fibroblasts. Invest Ophthalmol Vis Sci 2006, 47:1902–1910
67. Fujimura M, Morita-Fujimura Y, Noshita N, Sugawara T, Kawase M, Chan PH: The cytosolic antioxidant copper/zinc-superoxide dismutase prevents the early release of mitochondrial cytochrome c in ischemic brain after transient focal cerebral ischemia in mice. J Neurosci 2000, 20:2817–2824
68. Li Q, Sato EF, Zhu X, Inoue M: A simultaneous release of SOD1 with cytochrome c regulates mitochondria-dependent apoptosis. Mol Cell Biochem 2009, 322:151–159
69. Wallace DC: Mitochondrial diseases in man and mouse. Science 1999, 283:1482–1488
70. Hashizume K, Hirasawa M, Imamura Y, Noda S, Shimizu T, Shinoda K, Kurihara T, Noda K, Ozawa Y, Ishida S, Miyake Y, Shirasawa T, Tsubota K: Retinal dysfunction and progressive retinal cell death in SOD1-deficient mice. Am J Pathol 2008, 172:1325–1331
71. Methot N, Huang J, Coulombe N, Vaillancourt JP, Rasper D, Tam J, Han Y, Colucci J, Zamboni R, Xanthoudakis S, Toulmond S, Nicholson DW, Roy S: Differential efficacy of caspase inhibitors on apoptosis markers during sepsis in rats and implication for fractional inhibition requirements for therapeutics. J Exp Med 2004, 199:199–207
72. Perfettini JL, Kroemer G: Caspase activation is not death. Nat Immunol 2003, 4:308–310
73. Newton K, Strasser A: Caspases signal not only apoptosis but also antigen-induced activation in cells of the immune system. Genes Dev 2003, 17:819–825
74. Williams RM, Singh J, Sharkey KA: Innervation and mast cells of the rat exorbital lacrimal gland: the effects of age. J Auton Nerv Syst 1994, 47:95–108
75. Obata H, Yamamoto S, Horiuchi H, Machinami R: Histopathologic study of human lacrimal gland. Statistical analysis with special reference to aging. Ophthalmology 1995, 102:678–686
76. Draper CE, Adeghate E, Lawrence PA, Pallot DJ, Garner A, Singh J: Age-related changes in morphology and secretory responses of male rat lacrimal gland. J Auton Nerv Syst 1998, 69:173–183
77. Adeghate E, Draper CE, Singh J: Effects of ageing on changes in morphology of the rat lacrimal gland. Adv Exp Med Biol 2002, 506:103–107
78. Obata H: Anatomy and histopathology of the human lacrimal gland. Cornea 2006, 25:S82–S89
79. Damato BE, Allan D, Murray SB, Lee WR: Senile atrophy of the human lacrimal gland: the contribution of chronic inflammatory disease. Br J Ophthalmol 1984, 68:674–680
80. Tapinos NI, Polihronis M, Tzioufas AG, Skopouli FN: Immunopathology of Sjögren's syndrome. Ann Med Interne (Paris) 1998, 149:17–24
81. Manganelli P, Fietta P: Apoptosis and Sjögren syndrome. Semin Arthritis Rheum 2003, 33:49–65
82. Gyrd-Hansen M, Meier P: IAPs: from caspase inhibitors to modulators of NF-kappaB, inflammation and cancer. Nat Rev Cancer 2010, 10:561–574
83. Krabbe KS, Pedersen M, Bruunsgaard H: Inflammatory mediators in the elderly. Exp Gerontol 2004, 39:687–699
84. Fox RI, Kang HI, Ando D, Abrams J, Pisa E: Cytokine mRNA expression in salivary gland biopsies of Sjögren's syndrome. J Immunol 1994, 152:5532–5539
85. Narayanan S, Miller WL, McDermott AM: Conjunctival cytokine expression in symptomatic moderate dry eye subjects. Invest Ophthalmol Vis Sci 2006, 47:2445–2450
86. Tishler M, Yaron I, Geyer O, Shirazi I, Naftaliev E, Yaron M: Elevated tear interleukin-6 levels in patients with Sjögren syndrome. Ophthalmology 1998, 105:2327–2329
87. Jenny NS, Tracy RP, Ogg MS, Luong le A, Kuller LH, Arnold AM, Sharrett AR, Humphries SE: In the elderly, interleukin-6 plasma levels and the −174G>C polymorphism are associated with the development of cardiovascular disease. Arterioscler Thromb Vasc Biol 2002, 22:2066–2071
88. Bruunsgaard H, Benfield TL, Andersen-Ranberg K, Hjelmborg JB, Pedersen AN, Schroll M, Pedersen BK, Jeune B: The tumor necrosis factor alpha −308G>A polymorphism is associated with dementia in the oldest old. J Am Geriatr Soc 2004, 52:1361–1366
89. Bruunsgaard H, Ladelund S, Pedersen AN, Schroll M, Jorgensen T, Pedersen BK: Predicting death from tumour necrosis factor-alpha and interleukin-6 in 80-year-old people. Clin Exp Immunol 2003, 132:24–31
90. Bruunsgaard H, Pedersen BK: Age-related inflammatory cytokines and disease. Immunol Allergy Clin North Am 2003, 23:15–39
91. Thiery JP: Epithelial-mesenchymal transitions in tumour progression. Nat Rev Cancer 2002, 2:442–454
92. Radisky DC, Levy DD, Littlepage LE, Liu H, Nelson CM, Fata JE, Leake D, Godden EL, Albertson DG, Nieto MA, Werb Z, Bissell MJ: Rac1b and reactive oxygen species mediate MMP-3-induced EMT and genomic instability. Nature 2005, 436:123–127
93. Dasgupta P, Rizwani W, Pillai S, Kinkade R, Kovacs M, Rastogi S, Banerjee S, Carless M, Kim E, Coppola D, Haura E, Chellappan S: Nicotine induces cell proliferation, invasion and epithelial-mesenchymal transition in a variety of human cancer cell lines. Int J Cancer 2009, 124:36–45
94. Sullivan NJ, Sasser AK, Axel AE, Vesuna F, Raman V, Ramirez N, Oberyszyn TM, Hall BM: Interleukin-6 induces an epithelial-mesenchymal transition phenotype in human breast cancer cells. Oncogene 2009, 28:2940–2947
95. Asiedu MK, Ingle JN, Behrens MD, Radisky DC, Knutson KL: TGF{beta}/TNF{alpha}-mediated epithelial-mesenchymal transition generates breast cancer stem cells with a claudin-low phenotype. Cancer Res 2011, 71:4707–4719
96. Ogawa Y, Shimmura S, Kawakita T, Yoshida S, Kawakami Y, Tsubota K: Epithelial mesenchymal transition in human ocular chronic graft-versus-host disease. Am J Pathol 2009, 175:2372–2381
97. Mariette X: Pathophysiology of Sjögren's syndrome [in French]. Ann Med Interne (Paris) 2003, 154:157–168

98. Wallace DC: Mitochondrial DNA mutations in diseases of energy metabolism. J Bioenerg Biomembr 1994, 26:241–250
99. Goto E, Dogru M, Kojima T, Tsubota K: Computer-synthesis of an interference color chart of human tear lipid layer, by a colorimetric approach. Invest Ophthalmol Vis Sci 2003, 44:4693–4697
100. Nakamura S, Shibuya M, Nakashima H, Hisamura R, Masuda N, Imagawa T, Uehara M, Tsubota K: Involvement of oxidative stress on corneal epithelial alterations in a blink-suppressed dry eye. Invest Ophthalmol Vis Sci 2007, 48:1552–1558
101. Wakamatsu TH, Sato EA, Matsumoto Y, Ibrahim OM, Dogru M, Kaido M, Ishida R, Tsubota K: Conjunctival in vivo confocal scanning laser microscopy in patients with Sjögren's syndrome. Invest Ophthalmol Vis Sci 2010, 51:144–150
102. Okado-Matsumoto A, Fridovich I: Subcellular distribution of superoxide dismutases (SOD) in rat liver: Cu,Zn-SOD in mitochondria. J Biol Chem 2001, 276:38388–38393
103. Valentine JS, Doucette PA, Zittin Potter S: Copper-zinc superoxide dismutase and amyotrophic lateral sclerosis. Annu Rev Biochem 2005, 74:563–593
104. Henderson JW, Prough WA: Influence of age and sex on flow of tears. Arch Ophthal 1950, 43:224–231
105. Norn MS: Tear secretion in normal eyes. Estimated by a new method: the lacrimal streak dilution test. Acta Ophthalmol (Copenh) 1965, 43:567–573
106. McGill JI, Liakos GM, Goulding N, Seal DV: Normal tear protein profiles and age-related changes. Br J Ophthalmol 1984, 68:316–320

Modern Pathology (2012) 25, 956–967

Association between IgG4-related disease and progressively transformed germinal centers of lymph nodes

Yasuharu Sato[1], Dai Inoue[2], Naoko Asano[3], Katsuyoshi Takata[1], Hideki Asaoku[4], Yoshinobu Maeda[5], Toshiaki Morito[6], Hirokazu Okumura[7], Shin Ishizawa[8], Shoko Matsui[9], Takayoshi Miyazono[10], Tamotsu Takeuchi[11], Naoto Kuroda[12], Yorihisa Orita[13], Kiyoshi Takagawa[14], Masaru Kojima[15] and Tadashi Yoshino[1]

[1]*Department of Pathology, Okayama University Graduate School of Medicine, Dentistry and Pharmaceutical Sciences, Okayama, Japan;* [2]*Department of Radiology, Kanazawa University Graduate School of Medical Science, Kanazawa, Japan;* [3]*Department of Clinical Laboratory, Nagoya University Hospital, Nagoya, Japan;* [4]*Department of Clinical Laboratory, Hiroshima Red Cross Hospital and Atomic-Bomb Survivors Hospital, Hiroshima, Japan;* [5]*Department of Pathology, Toyama Red Cross Hospital, Toyama, Japan;* [6]*Department of Anatomic Pathology, Kagawa Rosai Hospital, Marugame, Japan;* [7]*Department of Internal Medicine, Toyama Prefectural Central Hospital, Toyama, Japan;* [8]*Department of Pathology, Toyama Prefectural Central Hospital, Toyama, Japan;* [9]*Department of First Internal Medicine, Graduate School of Medicine and Pharmaceutical Science, University of Toyama, Toyama, Japan;* [10]*Department of Gastroenterology and Hematology, Graduate School of Medicine and Pharmaceutical Science, University of Toyama, Toyama, Japan;* [11]*Department of Pathology, Kochi Medical School, Kochi, Japan;* [12]*Department of Diagnostic Pathology, Kochi Red Cross Hospital, Kochi, Japan;* [13]*Department of Otolaryngology, Head and Neck Surgery, Okayama University Graduate School of Medicine, Dentistry and Pharmaceutical Sciences, Okayama, Japan;* [14]*Department of Clinical Laboratory, Kurobe City Hospital, Kurobe, Japan and* [15]*Department of Anatomic and Diagnostic Pathology, Dokkyo University School of Medicine, Mibu, Japan*

Progressively transformed germinal centers is a benign condition of unknown pathogenesis characterized by a distinctive variant form of reactive follicular hyperplasia in lymph nodes. We recently reported Ig G4-related disease in progressively transformed germinal centers. However, no large case series has been reported and clinicopathologic findings remain unclear. Here, we report 40 Japanese patients (28 men, 12 women; median age, 56 years) with progressively transformed germinal centers of the lymph nodes who fulfilled the histological diagnostic criteria for IgG4-related disease (IgG4$^+$ progressively transformed germinal centers), with asymptomatic localized lymphadenopathy involving the submandibular nodes in 24, submandibular and cervical nodes in 14, cervical nodes only in 1, and cervical and supraclavicular nodes in 1. In all, 16 (52%) of 31 examined patients had allergic disease. Histologically, the lymph nodes demonstrated uniform histological findings, namely marked follicular hyperplasia with progressively transformed germinal centers, and localization of the majority of IgG4$^+$ plasma cells in the germinal centers. Serum IgG4, serum IgE and peripheral blood eosinophils were elevated in 87%, 92% and 53% of examined patients, respectively. Eighteen patients subsequently developed extranodal lesions (including five who developed systemic disease), which on histological examination were consistent with IgG4-related disease. IgG4$^+$ progressively transformed germinal centers presents with uniform clinicopathological features of asymptomatic localized submandibular lymphadenopathy, which persists and/or relapses, and sometimes progresses to extranodal lesions or systemic disease. Nine patients were administered steroid therapy when the lesions progressed, to which all

Correspondence: Dr Y Sato, MD, Department of Pathology, Okayama University Graduate School of Medicine, Dentistry, and Pharmaceutical Sciences, 2-5-1 Shikata-cho Kita-ku, Okayama 700-8558, Japan.
E-mail: satou-y@cc.okayama-u.ac.jp
Received 23 November 2011; revised 22 January 2012; accepted 22 January 2012; published online 6 April 2012

responded well. We suggest that IgG4$^+$ progressively transformed germinal centers should be included in the IgG4-related disease spectrum.
Modern Pathology (2012) **25,** 956–967; doi:10.1038/modpathol.2012.54; published online 6 April 2012

Keywords: IgG4-related disease; IgG4-related lymphadenopathy; PTGC

The term progressively transformed germinal centers was first used by Lennert and Müller–Hermelink to describe reactive follicular hyperplasia in the lymph nodes,[1] and progressively transformed germinal centers is observed in approximately 4% of patients with unspecific lymphadenopathy.[1–6] Germinal centers in affected lymph nodes are usually larger than regular germinal centers and composed mainly of mantle zone lymphocytes and remnants of germinal center cells. Although relapse is frequent, affecting about 20% of patients, progressively transformed germinal centers is considered a non-malignant condition.[2–6]

IgG4-related disease is a recently recognized syndrome characterized by mass-forming lesions with lymphoplasmacytic infiltration, accumulation of IgG4$^+$ plasma cells in affected tissues and increased serum IgG4 levels.[7–14] IgG4-related disease generally involves either localized or systemic lymph nodes,[8,13,14] and five histological subtypes of IgG4-related lymphadenopathy have been recognized.[8] In 2009, we were the first to report patients with IgG4-related disease in progressively transformed germinal centers of the lymph nodes (progressively transformed germinal centers-type IgG4-related lymphadenopathy).[14] Recently, while no large series has yet been reported, Grimm *et al*[15] included 14 cases with progressively transformed germinal centers in their series. However, clinicopathologic findings remain unclear.

Here, we report the clinicopathological characteristics of 40 cases of progressively transformed germinal centers of the lymph nodes that fulfill the histological diagnostic criteria for IgG4-related disease.

Materials and methods

Case Selection

Two of us (YS and TY) reviewed the Pathology Department database of our institution using the search terms 'progressively transformed germinal centers,' 'follicular hyperplasia' and 'lymph node' for the 13-year period from 1998 to 2011. In all, 62 cases of progressively transformed germinal centers were identified, 40 of which fulfilled the histological diagnostic criteria of IgG4-related disease, namely the presence of IgG4$^+$ plasma cells >100/high-power fields (HPFs) and IgG4$^+$/IgG$^+$ plasma cell ratio $>40\%$ (IgG4$^+$ progressively transformed germinal centers) (Table 1), whereas 22 did not (IgG4$^-$ progressively transformed germinal centers). The histological diagnostic criteria were outlined by the International Symposium on IgG4-RD (Boston, MA, USA, on 4–7 October 2011; http://www2.massgeneral.org/pathology/symposium/IgG4_related_systemic_dis.asp).

The clinical records and pathology materials of all cases were reviewed, and cases of multicentric Castleman's disease, malignant lymphoma or other lymphoproliferative disorders (including rheumatoid arthritis-related lymphadenopathy and other immune-mediated conditions, and so on) were histologically and clinically excluded.

Histological Examination and Immunohistochemistry

Surgically biopsied lymph node specimens were fixed in 10% formaldehyde and embedded in paraffin. Serial sections (4 μm) were cut from each paraffin-embedded tissue block, and several sections were stained with hematoxylin and eosin. Immunohistochemistry was performed on paraffin sections using an automated Bond Max stainer (Leica Biosystems, Melbourne, Australia). The primary antibodies used were as follows: IgG (polyclonal (1:10 000); Dako), IgG4 (HP6025 (1:400); The Binding Site), Kappa (NCL-KAP (1:100); Novocastra) and Lambda (NCL-LAM (1:200); Novocastra). The number of IgG4$^+$ or IgG$^+$ plasma cells was estimated for areas with the highest density of positive cells. Three different HPF ($\times 10$ in the eyepiece and $\times 40$ in the lens) in each section were counted, and the average number of positive cells per HPF was calculated.

Polymerase Chain Reaction for the Detection of Ig Heavy-Chain Gene Rearrangement

Ig heavy-chain gene rearrangement was analyzed by polymerase chain reaction performed according to standard procedures as described previously.[14] The primers used for Ig heavy-chain gene amplification were 5′-TGG[A/G]TCCG[C/A]CAG[G/C]C[T/C][T/C]C[A/C/G/T]GG-3′ as an upstream consensus V-region primer; 5′-TGAGGAGACGGTGACC-3′ as a consensus J-region primer; and 5′-GTGACCAGGGT[A/C/G/T]CCTTGGCCCCAG-3′ as a consensus J-region primer.[14]

Statistical Analysis

Differences in characteristics between the two groups were determined by the χ^2 test, Fisher's

Table 1 Clinical features of 40 patients with IgG4+ PTGC

No.	*Age/gender*	*Biopsy site (LN size, cm)*	*Initial presentation*	*Disease progression*	*Treatment (follow-up period, months)*	*Allergic disease*	*Eosinophil count in PB (%;nl<5%)*	*IgG4 (mg/dl; nl = 4.8–105)*	*IgG4/IgG (%; nl = 3–6)*	*IgE (IU/ml; nl) (IgE ratio)*[a]
1	36/M	Submandibular LN (1.5)	Bil. submandibular lymphadenopathy and lt. submandibular gland swelling	None (but residual lymph node lesions persisted)	Follow-up and stable (18)	Drug allergy	6.8	110	10.9	NA
2	75/M	Submandibular LN (3)	Bil. submandibular and cervical lymphadenopathy	NA	NA	NA	NA	NA	NA	NA
3	50/M	Submandibular LN (2)	Bil. submandibular and cervical lymphadenopathy	Residual lymph node lesions persisted and patient developed bil. axillary lymphadenopathy 3 years later	Follow-up (18)	Allergic rhinitis	21.1	183	6.74	NA
4	50/F	Submandibular LN (1.5)	Bil. submandibular lymphadenopathy	None (but residual lymph node lesions persisted)	Follow-up and stable (4)	Allergic rhinitis	2	24	2	NA
5	66/M	Submandibular LN (2)	Lt. submandibular lymphadenopathy	Relapsed lt. submandibular lymphadenopathy 10 months later[b]	Follow-up (10)	None	5.9	314[c]	19.2[c]	505 (2.9)
6	46/M	Submandibular LN (3.5)	Lt. submandibular lymphadenopathy, lt. submandibular gland swelling and thickened rt. pleura	None (but residual lymph node lesions persisted)	Follow-up and stable (10)	NA	3	NA	NA	NA
7	71/M	Submandibular LN (1.5)	Lt. submandibular and cervical lymphadenopathy	None (but residual lymph node lesions persisted)	Follow-up and stable (5)	None	2.5	275	12.8	259 (1.5)
8	62/F	Submandibular LN (1.5)	Lt. submandibular lymphadenopathy	None	Follow-up and stable (6)	Contact dermatitis	0	NA	NA	NA
9	75/F	Cervical and supraclavicular LN (2)	Rt. cervical and supraclavicular lymphadenopathy	None (the cervical LN was biopsied 9 months ago but a residual supraclavicular lymph node lesion persisted)	Follow-up and stable (10)	Food allergy	8	36.2	2.3	47.0 (0.27)
10	45/F	Cervical LN (3)	Lt. cervical lymphadenopathy	Residual lymph node lesions persisted; LN size increased in 3 years	Follow-up (36)	Asthma and drug allergy	7	NA	NA	NA
11	64/M	Submandibular LN (3)	Rt. submandibular lymphadenopathy	Relapsed rt. submandibular lymphadenopathy[b] 2 years later; patient developed bil. lacrimal,[b] parotid, and submandibular gland swelling, mediastinal lymphadenopathy, and kidney lesion[b] 11 years later	Steroid therapy was performed when disease progressed, with good response (144)	Asthma, drug allergy and allergic rhinitis	10.5	2550[c]	42.3[c]	NA
12	60/M	Submandibular LN (2)	Lt. submandibular and cervical lymphadenopathy	NA	NA	None	2.2	NA	NA	NA

Table 1 Continued

No.	*Age/gender*	*Biopsy site (LN size, cm)*	*Initial presentation*	*Disease progression*	*Treatment (follow-up period, months)*	*Allergic disease*	*Eosinophil count in PB (%;nl<5%)*	*IgG4 (mg/dl; nl = 4.8–105)*	*IgG4/IgG (%; nl = 3–6)*	*IgE (IU/ml; nl) (IgE ratio)*[a]
13	61/M	Submandibular LN (2)	Lt. submandibular lymphadenopathy	Developed bil. submandibular gland swelling, mediastinum, lung, pancreas kidney and aortic lesions 3 years later	Steroid therapy was performed when disease progressed, with good response (101)	None	4	2240[c]	77.5[c]	NA
14	43/F	Submandibular LN (1)	Rt. submandibular and cervical lymphadenopathy	NA	NA	NA	NA	NA	NA	NA
15	46/M	Submandibular LN (3)	Lt. submandibular lymphadenopathy	Relapsed lt. submandibular LN 5 years later[b] Relapsed rt. submandibular LN 8 years later.[b]	Follow-up (100)	None	7.7	40	2.6	681 (1.9)
16	58/F	Submandibular LN (1.5)	Rt. submandibular lymphadenopathy	Developed bil. submandibular gland swelling 1 year later[b] and bil. lacrimal gland swelling 4 years later	Follow-up (48)	Contact dermatitis	2.2	241[c]	18.4[c]	280[c] (1.6)
17	55/M	Submandibular LN (3)	Rt. submandibular and cervical lymphadenopathy	None (but residual lymph node lesions persisted)	Follow-up and stable (6)	None	4.1	NA	NA	NA
18	52/F	Submandibular LN (2.5)	Lt. submandibular and cervical lymphadenopathy	None (but residual lymph node lesions persisted)	Follow-up and stable (3)	NA	4	NA	NA	NA
19	51/F	Submandibular LN (2)	Rt. submandibular lymphadenopathy	Developed bil. submandibular lymphadenopathy and rt. parotid gland swelling 1 year later[b]	Follow-up (18)	None	NA	224	NA	NA
20	52/M	Submandibular LN (2.5)	Lt. submandibular lymphadenopathy	Developed bil. lacrimal gland swelling, skin lesion and systemic lymphadenopathy 5 years later[b]	Steroid therapy was performed when disease progressed, with good response. However, the lesion relapsed 3 months later (96)	None	14[c]	1700[c]	37.5[c]	904[c] (2.5)
21	43/M	Submandibular LN (2)	Lt. submandibular lymphadenopathy	Developed bil. lacrimal gland swelling, skin lesion and systemic lymphadenopathy 3 years later[b]	Steroid therapy was performed when disease progressed, with good response. However, the lesion relapsed 3 years later (78)	Atopic dermatitis	9	216[c]	13.72[c]	1550[c] (4.3)

Table 1 Continued

No.	Age/gender	Biopsy site (LN size, cm)	Initial presentation	Disease progression	Treatment (follow-up period, months)	Allergic disease	Eosinophil count in PB (%;nl<5%)	IgG4 (mg/dl; nl = 4.8–105)	IgG4/IgG (%; nl = 3–6)	IgE (IU/ml; nl) (IgE ratio)[a]
22	58/M	Submandibular LN (2)	Bil. submandibular and cervical lymphadenopathy	Developed prostatic lesion and systemic lymphadenopathy 2 years later[b]	Steroid therapy was performed when disease progressed, with good response. However, the lesion relapsed 10 months later (39)	Drug allergy	8	1280[c]	30.74[c]	641[c] (1.8)
23	50/M	Submandibular LN (1)	Bil. submandibular lymphadenopathy	None	Follow-up and stable (36)	None	4	NA	NA	NA
24	45/F	Submandibular LN (2.5)	Rt. submandibular and cervical lymphadenopathy	Developed bil. lacrimal gland swelling 1 year later	Steroid therapy was performed when disease progressed, with good response (16)	None	4	NA	NA	800 (2.2)
25	67/M	Submandibular LN (3)	Bil. submandibular lymphadenopathy	None (but residual lymph node lesions persisted)	Follow-up and stable (72)	NA	8.2	NA	NA	NA
26	51/F	Submandibular LN (3.5)	Rt. submandibular lymphadenopathy and rt. submandibular gland swelling	None	Follow-up and stable (12)	None	2.8	NA	NA	NA
27	42/M	Submandibular LN (2)	Lt. submandibular and cervical lymphadenopathy	None (but residual lymph node lesions persisted)	Follow-up and stable (60)	None	6.1	NA	NA	241 (1.4)
28	49/M	Submandibular LN (2.5)	Lt. submandibular, cervical lymphadenopathy, and lt. submandibular gland swelling	NA	NA	NA	1	NA	NA	NA
29	58/M	Submandibular LN (2.5)	Rt. submandibular lymphadenopathy	Developed bil. lacrimal gland swelling and rt. maxillary sinus tumor 3 years later[b]	Steroid therapy was performed when disease progressed, with good response (39)	Allergic rhinitis	9	921[c]	47.5[c]	1090[c] (3.0)
30	60/M	Submandibular LN (2.5)	Rt. submandibular lymphadenopathy	None	Follow-up and stable (26)	Asthma	3	NA	NA	NA
31	46/F	Submandibular LN (2)	Rt. submandibular lymphadenopathy and rt. submandibular gland swelling	NA	NA	Allergic rhinitis	NA	NA	NA	NA
32	72/M	Submandibular LN (2.5)	Bil. submandibular lymphadenopathy	None (but residual lymph node lesions persisted)	Follow-up and stable (12)	NA	0.4	NA	NA	NA

Table 1 Continued

No.	*Age/gender*	*Biopsy site (LN size, cm)*	*Initial presentation*	*Disease progression*	*Treatment (follow-up period, months)*	*Allergic disease*	*Eosinophil count in PB (%;nl<5%)*	*IgG4 (mg/dl; nl = 4.8–105)*	*IgG4/IgG (%; nl = 3–6)*	*IgE (IU/ml; nl) (IgE ratio)*[a]
33	51/M	Submandibular LN (3.5)	Rt. submandibular and cervical lymphadenopathy	None (but residual lymph node lesions persisted)	Follow-up and stable (26)	Allergic rhinitis	6.7	169	7	3250 (18.8)
34	68/F	Submandibular LN (1.5)	Rt. submandibular lymphadenopathy and rt. lacrimal gland swelling	None (but residual lymph node lesions persisted)	Follow-up and stable (25)	Food and drug allergy	5.6	NA	NA	NA
35	67/M	Submandibular LN (2)	Lt. submandibular lymphadenopathy	None	Follow-up and stable (27)	Allergic rhinitis and asthma	NA	NA	NA	NA
36	70/M	Submandibular LN (2)	Lt. submandibular lymphadenopathy and lt. parotid gland[b] tumor	Developed rt. submandibular gland swelling and pancreatic lesion[b] 2 years later	Steroid therapy was performed when disease progressed, with good response (43)	NA	10.9	483[c]	27.7[c]	NA
37	51/M	Submandibular LN (1.5)	Rt. submandibular, cervical lymphadenopathy, and bil. submandibular gland swelling	None (but residual lymph node lesions persisted)	Follow-up and stable (18)	None	6.3	NA	NA	NA
38	61/M	Submandibular LN (2)	Bil. submandibular and cervical lymphadenopathy	NA	NA	NA	2.6	NA	NA	NA
39	76/M	Submandibular LN (1.5)	Rt. submandibular lymphadenopathy	Developed skin lesion[b] and bil. lacrimal gland swelling 2 years later	Steroid therapy was performed on bil. swelling of the lacrimal gland, with good response (63)	Asthma	11.6	NA	NA	875 (2.4)
40	57/M	Submandibular LN (3)	Rt. submandibular lymphadenopathy	Relapsed rt. submandibular lymphadenopathy 2 and 8 years later[b]	Follow-up (97)	None	NA	NA	NA	NA

Abbreviations: Bil., bilateral; LN, lymph node; lt., left; NA, not available; nl, normal; PB, peripheral blood; PTGC, progressively transformed germinal centers; rt., right.
[a]IgE ratio: measured value/normal value.
[b]The lesion was histologically diagnosed as IgG4-related disease.
[c]The data was obtained at relapse or disease progression time.

Table 2 Summary of clinical features of IgG4+ PTGC

Number	40
Gender	
Male/female	28/12
Age	
Median (range)	56 (36–76)
≥60	16 (40%)
Allergic disease history	16/31 (51.6%)
Laboratory findings	
Increased eosinophil count in peripheral blood	18/34 (52.9%)
Elevated serum IgG4 level	14/17 (82.4%)
Elevated serum IgE level	12/13 (92.3%)
Initial lymphadenopathy	
Submandibular lymphadenopathy	24 (bilateral; 5)
Submandibular and cervical lymphadenopathy	14 (bilateral; 4)
Cervical lymphadenopathy	1 (unilateral)
Cervical and supraclavicular lymphadenopathy	1 (unilateral)
Number of available follow-up reports	34
Follow-up period	
Median (range)	26 (3–144)
Persistence or relapse of lymph node lesions	23/34 (67.6%)
Progression to extranodal lesions	18/34 (52.9%)
Submandibular gland	5
Lacrimal gland	2
Lacrimal gland and submandibular gland	1
Lacrimal gland and skin	3
Submandibular gland and pleura	1
Lacrimal gland and maxillary sinus	1
Lacrimal gland, submandibular gland, parotid gland, mediastinum, kidney	1
Submandibular gland, mediastinum, lung, pancreas, aorta, kidney	1
Submandibular gland and parotid gland	1
Parotid gland	1
Prostate	1
Progression to systemic lymphadenopathy	3/34 (8.8%)

Abbreviation: PTGC, progressively transformed germinal centers.

exact test, Student's *t*-test or Mann–Whitney *U*-test, as appropriate. All data were analyzed with the STATA software (version 10.0; Stata, College Station, TX, USA).

Results

Clinical Features of IgG4+ Progressively Transformed Germinal Centers

Clinical findings are summarized in Tables 1 and 2. There were 28 men and 12 women with a median age of 56 years (range, 36–76 years). On initial clinical examination, all patients presented with localized submandibular and/or cervical, or cervical and supraclavicular lymphadenopathy. Twenty-four patients showed submandibular lymphadenopathy, which was bilateral in five. Fourteen patients showed submandibular and cervical lymphadenopathy, which was bilateral in four. Only two patients showed cervical, or cervical and supraclavicular lymphadenopathy. In total, 38 (95%) of 40 patients showed submandibular lymphadenopathy. Lymph node biopsy revealed that the size of the biopsied lymph nodes ranged from 1 to 3.5 cm in diameter, with an average of 2.2 cm. In addition, ^{18}F-fluorodeoxy glucose positron emission tomography showed significantly elevated uptake in examined patients (Figure 1). The lesions were therefore all suspected to be malignant lymphomas at initial clinical diagnosis.

Among patients examined for each respective factor, allergic disease was identified in 16 (52%) of 31 patients; peripheral blood eosinophil count was increased in 18 (53%) of 34; serum IgG4 levels were elevated in 14 (82%) of 17; and serum IgE levels were elevated in 12 (92%) of 13.

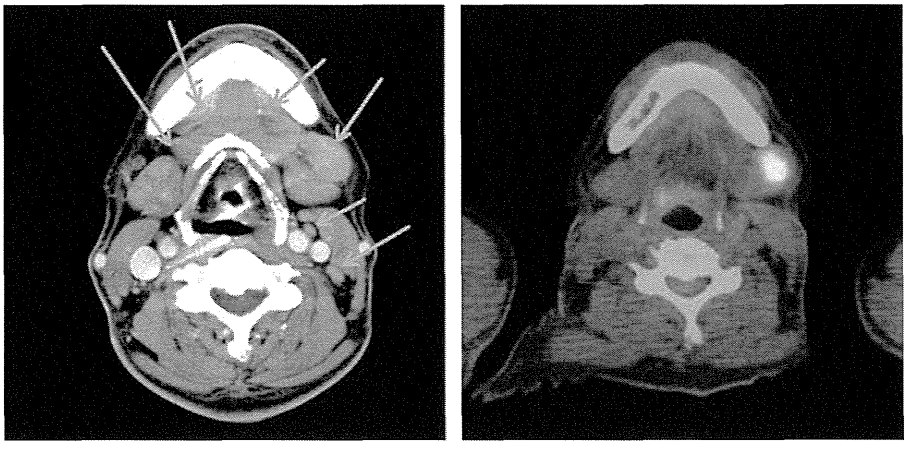

Figure 1 Ragiological images of IgG4+ progressively transformed germinal centers. Patient no. 12 had localized left submandibular lymphadenopathy and cervical lymphadenopathy (left panel). ^{18}F-fluorodeoxy glucose positron emission tomography showed significantly elevated uptake in the left submandibular lymph node (right panel). The lesion was radiologically and clinically suspected to be malignant lymphoma.

Table 3 Clinicopathological characteristics of patients with IgG4$^+$PTGC and IgG4$^-$PTGC

	IgG4$^+$PTGC (n = *40*)	*IgG4$^-$PTGC* (n = *22*)	P[a]
Gender			
(Male/female)	28/12	13/9	0.39
Age (years)			
Median	56	47	0.060
Mean (range)	56.5 (36–76)	46.6 (18–78)	
>40 years old	39 (98%)	14 (64%)	<0.0001
>50 years old	30 (75%)	10 (45%)	0.02
Lymphadenopathy area			
Submandibular LN	38 (95%)	1 (4.5%)	<0.0001
Cervical LN	16 (40%)	11 (50%)	0.45
Supraclavicular LN	1 (2.5%)	1 (4.6%)	0.66
Axillary LN	0 (0%)	6 (27%)	0.001
Paraaortic LN	0 (0%)	2 (9%)	0.053
Inguinal LN	0 (0%)	5 (23%)	0.002
IgG4$^+$/IgG$^+$ plasma cell ratio			
Mean	57.4	5.0	
Median (range)	57.8 (44.2–78.1)	3.7 (0–16.7)	<0.0001

Abbreviations: LN, lymph node; PTGC, progressively transformed germinal centers.
[a]IgG4$^+$PTGC *vs* IgG4$^-$PTGC.

Clinicopathological Differences Between IgG4$^+$ Progressively Transformed Germinal Centers and IgG4$^-$ Progressively Transformed Germinal Centers

The clinicopathological findings associated with 40 cases of IgG4$^+$ progressively transformed germinal centers and 22 of IgG4$^-$ progressively transformed germinal centers (IgG4$^+$/IgG$^+$ plasma cell ratio $\leq$40%) are summarized in Table 3, Supplementary Figure 1 and Supplementary Table 1. Lymph nodes affected by IgG4$^+$ progressively transformed germinal centers showed a markedly elevated IgG4$^+$/IgG$^+$ plasma cell ratio compared with those with IgG4$^-$ progressively transformed germinal centers (mean 57% *vs* 5%, $P<0.0001$). Patients with IgG4$^+$ progressively transformed germinal centers showed an older age distribution and a higher incidence of submandibular lymph node involvement than those with IgG4$^-$ progressively transformed germinal centers ($P<0.0001$).

Pathological Findings in IgG4$^+$ Progressively Transformed Germinal Centers

In patients with IgG4$^+$ progressively transformed germinal centers, the lymph nodes demonstrated numerous lymphoid follicles with hyperplastic germinal centers and a distinct mantle zone, but no expansion of the interfollicular zone. Progressively transformed germinal centers were observed in all cases, appearing as round to oval structures 2–3 times the diameter of the other reactive follicles and composed predominantly of small lymphocytes, centrocytes, centroblasts, and numerous mature plasma cells and plasmacytoid cells. The interfollicular zone showed infiltration of a significant number of eosinophils, and T-zones were indistinct (Figure 2).

Interestingly, a unique feature of IgG4$^+$ progressively transformed germinal centers on immunohistochemistry was the localization of the majority of IgG4$^+$ plasma cells in the germinal centers, with only a small number present in the interfollicular zone (Figure 2), except in case no. 3, where they were detected in both the germinal centers and interfollicular zone. The IgG4$^+$ plasma cells were >100/HPF and IgG4$^+$/IgG$^+$ plasma cell ratio was >40% in all cases (Table 3 and Supplementary Figure 1B). Immunoglobulin light-chain restriction was not detected in any case. These histological and immunohistochemical findings were all compatible with progressively transformed germinal centers-type IgG4-related lymphadenopathy.[8,14]

In contrast, the lymph nodes of patients with IgG4$^-$ progressively transformed germinal centers showed heterogenous histological findings, demonstrating a small number or numerous lymphoid follicles with or without hyperplastic germinal centers, and expansion or no expansion of the interfollicular zone. The interfollicular zone did not show a significant number of eosinophils, and T-zones were distinct. IgG4$^+$ plasma cells were absent or few, and the IgG4$^+$/IgG$^+$ plasma cell ratio was <40% in all cases.

Disease Progression and Extranodal Lesions in IgG4$^+$ Progressively Transformed Germinal Centers

Thirty-four patients were followed by regular imaging, laboratory findings and clinical evaluation over 3 to 144 months (median, 26 months). During the follow-up period, 23 (68%) patients showed persistence or relapse (or both) of these residual lymph nodes. In all, 18 patients progressed to the development of extranodal lesions, of whom 16 (89%) interestingly showed the involvement of lacrimal and/or submandibular glands. Moreover, 5 of these 18 patients showed progression to systemic disease (Table 2 and Figure 3; patient nos. 11, 13, 20, 21 and 22). Histologically examined extranodal lesions were consistent with IgG4-related disease.

Clinical Management of IgG4$^+$ Progressively Transformed Germinal Centers

In all, 18 of the 34 patients showed stable disease, despite the presence of persistent residual lymph node lesions in almost all. Ten patients showed the localized or systemic relapse of lymphadenopathy, and were re-biopsied. Nine patients were administered steroid therapy when the lesions progressed, to which all responded well (Table 1).

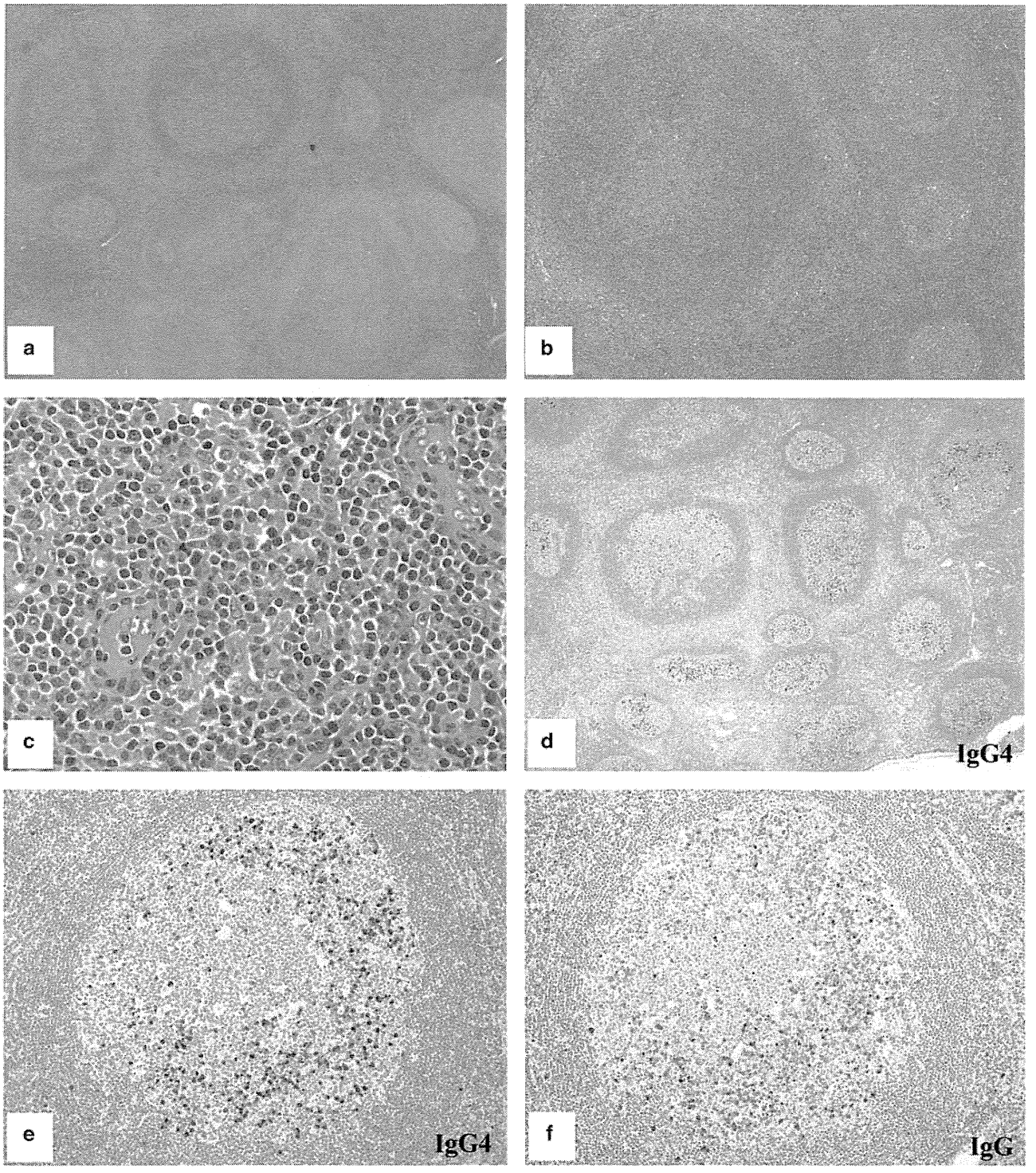

Figure 2 Histological and immunohistochemical features of IgG4$^+$ progressively transformed germinal centers. (**a**, **b**) Lymph nodes from patient no. 26 showed numerous lymphoid follicles with hyperplasia and progressively transformed germinal centers (hematoxylin and eosin, **a**: × 20). (**b**) The progressively transformed germinal centers were appearing as round to oval structures 2–3 times the diameter of the other reactive follicles (hematoxylin and eosin, × 40). (**c**) Abundant eosinophil infiltration in the interfollicular zone (hematoxylin and eosin, × 200). (**d**) Localization of the majority of IgG4$^+$ plasma cells in the germinal centers (IgG4-immunostaining, × 20). (**e**, **f**) The IgG4$^+$/IgG$^+$ plasma cell ratio was >60% (IgG4 and IgG-immunostaining, × 100).